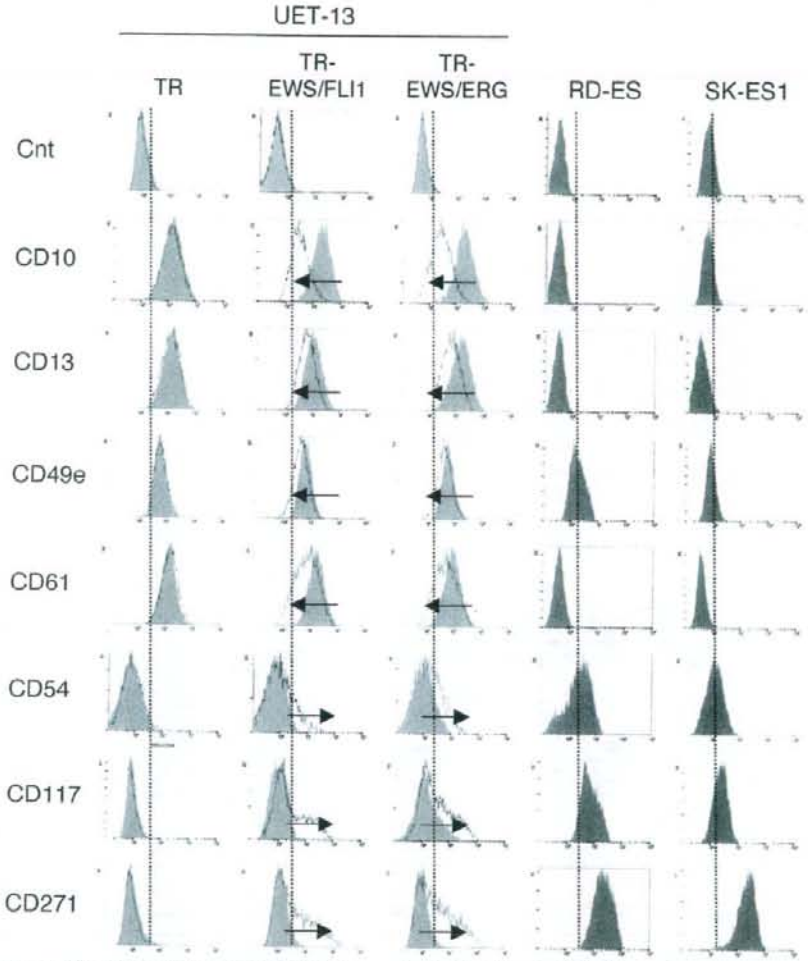

FIG. 5. Immunophenotypic change on induction of EWS/ETS expression in UET-13 cells. UET-13 transfectants were cultured with or without 3 μg/ml of tetracycline for 1 week and flow cytometric analyses were performed by using a set of antibodies as indicated. The histograms of UET-13 transfectants with (empty) and without (gray) tetracycline treatment were overlaid. Dotted lines indicate fluorescence intensities in negative control panels (Cnt). Arrows indicate the immunophenotypic change caused by tetracycline. The immunophenotypes of the EFT cell lines RD-ES and SK-ES1 were also examined.

controlled at the transcriptional level in the presence of EWS/ETS.

We next investigated the candidate genes whose expression is regulated by EWS/ETS in human MPCs. First, we selected the genes with up-regulated or down-regulated expression by EWS/ETS induction using gene cluster analysis (Fig. 7A; UET-13TR-EWS/FLI1 up, 4,294 probes; down, 4,103 probes; UET-13TR-EWS/ERG up, 3,358 probes; down, 3,705 probes). To reduce the number of the candidate genes, we selected up-regulated genes that are expressed in tetracycline-treated cells at least 1.5-fold higher than in untreated cells (UET-13TR-EWS/FLI1, 1,137 probes; UET-13TR-EWS/ERG, 835 probes). Similarly, the down-regulated genes that are expressed in tetracycline-treated cells at least 0.75-fold lower than in untreated cells (UET-13TR-EWS/FLI1, 1,803 probes; UET-13TR-EWS/ERG, 773 probes). By selecting common probes in both cells, we finally identified a group of candidate genes significantly controlled by EWS/ETS induction in the human mesenchymal progenitor background. Since microarray analysis was performed as a global screening in a single experiment, it is likely that there is a fair bit of noise in the derived gene profiles due to the lack of replicate data. This may account in part for the limited overlap between the profiles induced by EWS-FLI1 and EWS-ERG, whereas we still identified 349 probes of common up-regulated genes and 293 probes of common down-regulated genes (see the supplemental material). In addition to the EFT-specific genes mentioned above, these contained those previously described as EFT-specific genes, such as those for OB-cadherin/cadherin-11 (31), Janus

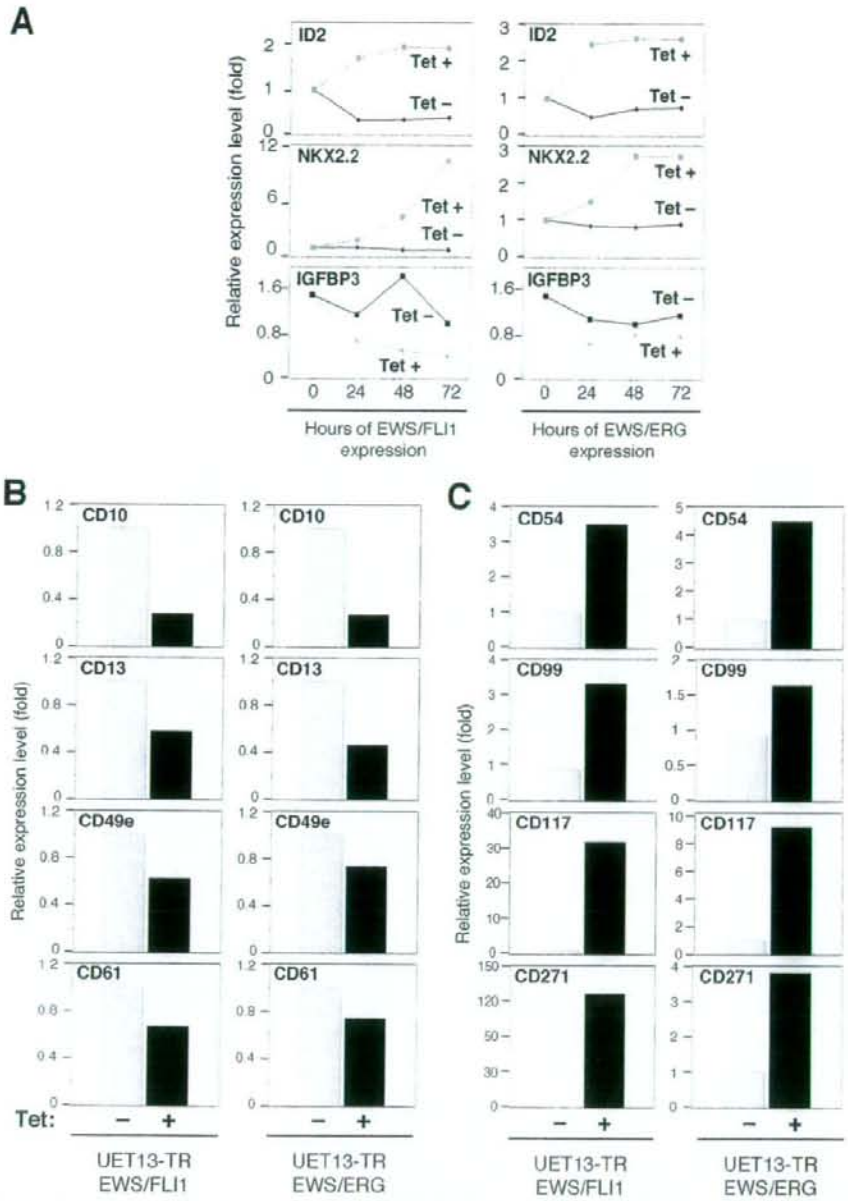

FIG. 6. The change of expression profile on induction of EWS/ETS in UET-13 cells. UET-13TR-EWS/FLI1 and UET-13TR-EWS/ERG cells were cultured in the absence or presence of tetracycline (Tet) for the indicated periods and analyzed using the Affymetrix human genome U133 Plus 2.0 array as described in Materials and Methods. (A) The sequential changes of ID2, NKX2.2, and IGFBP3 mRNA levels in UET-13 transfectants upon treatment with or without tetracycline. Diamond symbols indicate UET-13 transfectants in the absence of tetracycline; box symbols indicate UET-13 transfectants in the presence of tetracycline. (B and C) Microarray studies for the determination of expression profiles of surface antigens in UET-13 transfectants. UET-13 transfectants were treated with or without 3 μg/ml of tetracycline for 72 h. mRNA levels were determined with the Affymetrix human genome U133 Plus 2.0 array.

kinase 1 (JAK1) (49), keratin 18, and six-transmembrane epithelial antigen of the prostate (STEAP) (22). The expression pattern of these genes (642 probes) in UET-13 transfectants in the absence or presence of tetracycline is shown in the gene cluster in Fig. 7B. The expression of these genes was indeed changed significantly after EWS/ETS expression in both cells. They included genes associated with signal transduction (such as those for epidermal growth factor receptor, FAS [CD95], and fibroblast

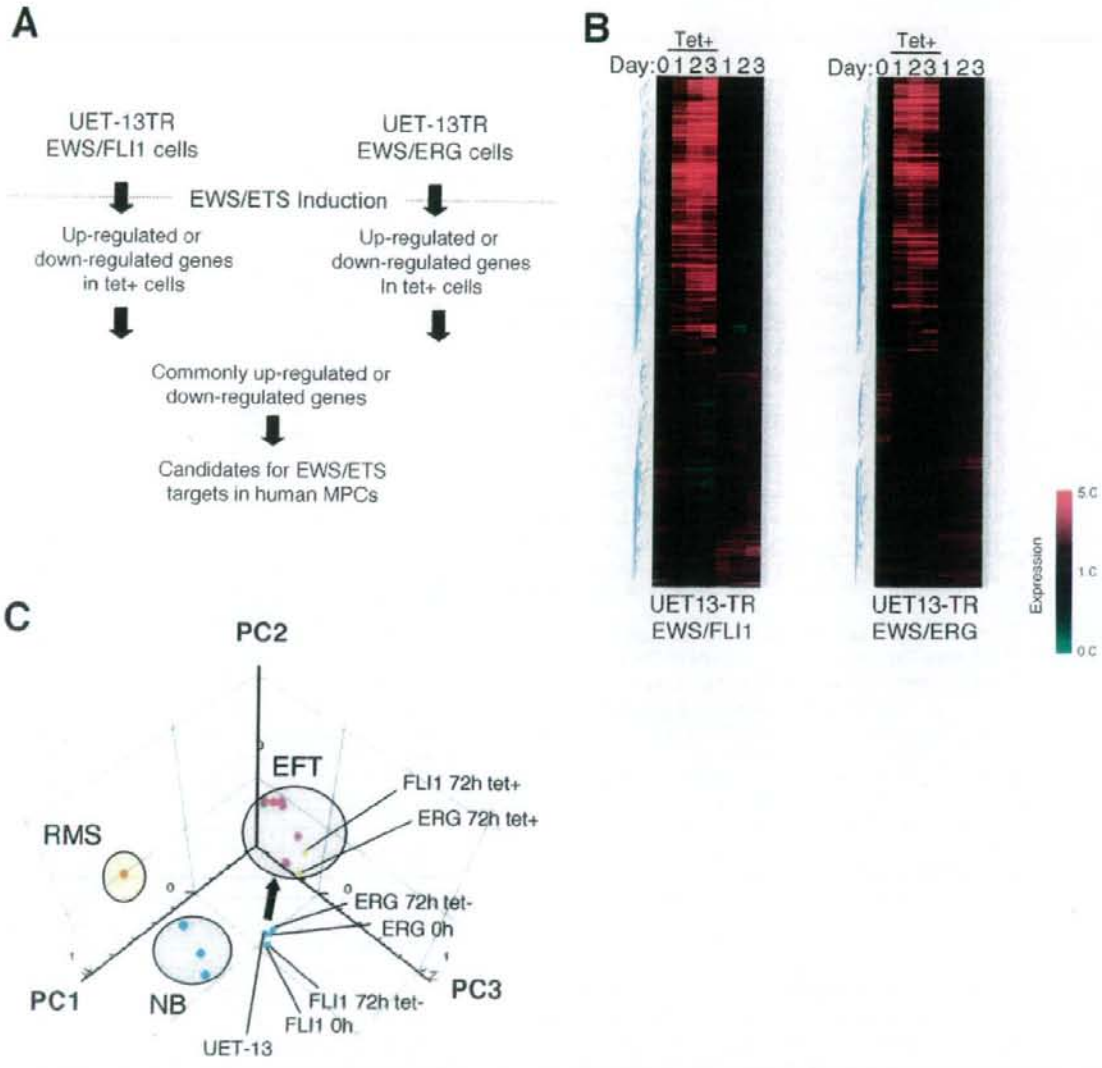

FIG. 7. Identification of candidates for the target of EWS/ETS in human MPCs by use of a microarray. UET-13TR-EWS/FLI1 and UET-13TR-EWS/ERG cells were cultured as described for Fig. 6 and analyzed using the Affymetrix human genome U133 Plus 2.0 array as described in Materials and Methods. (A) Scheme for the analysis of microarray data. (B) Gene cluster analysis of UET-13 transfectants in the absence or presence of tetracycline by use of 642 candidate genes for targets of EWS/ETS in human MPCs. (C) Visualization of sequential change by the gene expression profile in UET-13 transfectants following tetracycline-mediated EWS/ETS expression based on a PCA of 642 candidate genes. Deep blue plots indicate UET-13 cells. Light blue plots indicate UET-13 transfectants in the absence of tetracycline for 72 h. Yellow plots indicate UET-13 transfectants in the presence of tetracycline for 72 h. The pink circle indicates EFT cell lines expressing EWS/FLI1 (purple plots), EWS/ERG (red plot), and EWS/E1AF (light green plot). The light blue circle with blue plots indicates NB cell lines. The yellow circle with an orange plot indicates a rhabdomyosarcoma (RMS) cell line. Cutoff induction and repression levels are 1.5-fold and 0.75-fold, respectively. Tet, tetracycline.

growth factor receptor 1) and development (such as jagged-1 and frizzled-4, -7, and -8). Interestingly, in addition to the surface antigens presented in Fig. 6B and C, the expression profiling of EWS/ETS-expressing UET-13 cells displayed the modulation of several genes associated with cell adhesion, cytoskeletal structure, and membrane trafficking, such as those for collagen-11 and -21, ephrin receptor-A2, -B2, and -B3, ephrin-B1, claudin-1, integrin-α11, -αM, and -β2, CD66 (carcinoembryonic antigen-related cell adhesion molecule-1), and CD102 (intercellular cell adhesion molecule-2). They also included genes of chemokines CCL-2 and -3. These data raise the possibility that EWS/ETS can contribute to the membrane condition in human MPCs via the regulation of these cell surface molecules and chemokines.

Using these genes, we performed a PCA to visualize the shift in the gene expression pattern among the 642 probes. As shown in Fig. 7C, the plots of UET-13 transfectants treated with tetracycline became closer to those of EFT cells than to those of UET-13 transfectants without tetracycline treatment. These results indicated that the expression pattern of these genes was altered from that of UET-13 cells to that of EFT cells in an EWS/ETS-dependent manner. Since the gene expression profile of UET-13 cells is similar to those of other cell types of mesenchymal origin (data not shown), our results highlighted that the phenotypic alteration from mesenchyme to EFT-like cells in UET-13 cells induced by tetracycline treatment was accompanied by a change in the global gene expression profile.

EWS/ETS expression enhances the Matrigel invasion of UET-13 cells. To assess the role of EWS/ETS in malignant transformation in human MPCs, UET-13 transfectants were examined by invasion assay. As shown in Fig. 8A, tetracycline treatment did not affect the Matrigel invasion ability of UET-13TR cells. When examined similarly, however, tetracycline treatment resulted in an apparently increased invasion ($P < 0.05$) for both UET-13TR-EWS/FLI1 (Fig. 8B) and UET-13TR-EWS/ERG (Fig. 8C) cells. The results indicated that EWS/ETS expression can induce Matrigel invasion properties in human MPCs.

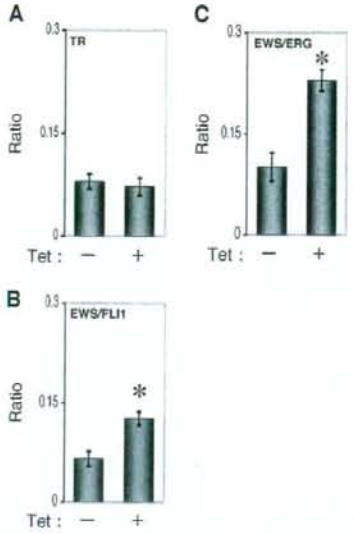

FIG. 8. Effects of EWS/ETS expression on the Matrigel invasion ability of UET-13 cells. UET-13TR (A), UET-13TR-EWS/FLI1 (B), and UET-13TR-EWS/ERG (C) cells were cultured in the absence or presence of tetracycline (Tet) for 72 h and then plated (2.5×10^4) on Matrigel-coated or uncoated filter inserts. After 20 h of culture, invading cells were stained with hematoxylin-eosin and counted in five fields per membrane as described in Materials and Methods. *, $P < 0.05$.

DISCUSSION

In the present study, using UET-13 cells as a model of human MPCs, we demonstrated that ectopic expression of EWS/ETS promoted the acquisition of an EFT-like phenotype, including cellular morphology, immunophenotype, and gene expression profile. Moreover, EWS/ETS expression enhances the ability of UET-13 cells to invade Matrigel. This assay is thought to mimic the early steps of tumor invasion in vivo (34), and the ability to penetrate the Matrigel has been positively correlated with invasion potential in several studies. Therefore, we concluded that EWS/ETS expression could mediate a part of the feature of tumor transformation in human MPCs. Thus, our culture system would provide a good model for testing the effects of EWS/ETS in human MPCs.

Several lines of evidence have indicated the transforming ability of EWS/FLI1, whereas that of EWS/ERG is not yet to be clarified. Therefore, it is noteworthy that our data demonstrated that EWS/ERG could promote an EFT-like phenotype in UET-13 cells similarly to EWS/FLI1. Thus, EWS/ERG also has the ability to induce an EFT-like phenotype in the human system. The major steps in the development of EFT should be commonly regulated by distinct chimeric EWS/ETS proteins. Indeed, several genes are common transcriptional targets of different chimeric EWS/ETS proteins in the murine system (11, 24, 35). Our data also showed that the 642 probes are coregulated in both EWS/FLI1-expressing cells and EWS/ERG-expressing cells. Further comparative studies of both the EWS/FLI1- and the EWS/ERG-mediated onset of EFT could allow us to understand the common functions of EWS/FLI1 and EWS/ERG in EFT. In addition, our systems are also useful for precisely distinguishing between the functions of these chimeric molecules in the development of EFT.

As mentioned above, the immunophenotypic analysis also revealed that the expression profiles of surface antigens in UET-13 cells were changed in favor of EFT cells in the presence of EWS/ETS (Fig. 4). Notably, the expression of CD54 (intercellular cell adhesion molecule-1 [ICAM1]), CD117 (c-kit), and CD271 (low-affinity nerve growth factor receptor [LNGFR]) increased in EWS/ETS-expressing UET-13 cells. These markers are positive in EFT cell lines (17, 28, 33), and in addition, CD117 is detected in about 40% of patient samples (17) and is negative in human primary MPCs (4, 43). Thus, it is reasonable to consider that a phenotypic marker of EFT was induced in UET-13 cells by EWS/ETS expression. On the other hand, CD54 and CD271 are positive in human primary MPCs (8, 25, 42), whereas these markers are negative in UET-13 cells. However, a previous report showed the disappearance of some positive markers, including CD271, from primary human MPCs during the process of ex vivo expansion

(25), and it has been speculated that the expression of these molecules in MPCs is induced in vivo via interaction with the bone marrow microenvironment and that the necessary stimuli are absent from ex vivo culture conditions. Therefore, the immunophenotype of UET-13 cells rather might be related to that of ex vivo-expanded primary human MPCs. In addition, it may be possible that EWS/ETS expression led to the reexpression of these disappeared markers in UET-13 cells without the necessary stimuli. In this case, the maintenance of CD271 expression outside of the bone marrow microenvironment might be a characteristic of EFT. Thus, our results proved that both EWS/FLI1 and EWS/ERG can be major causes of the expression of these markers and that human MPCs that precisely recapitulate the expression are strong candidates for the cell origins of EFT cells. The findings also imply that these antigens are suitable targets for diagnostic tools and new therapeutic agents. In fact, imatinib mesylate, which demonstrates anticancer activity against malignant cells expressing BCR-ABL as well as CD117 and platelet-derived growth factor receptor, inhibits proliferation and increases sensitivity to vincristine and doxorubicin in EFT cells (17).

Notably, our results also indicate that UET-13 cells, which have the MPC phenotype, possess the potential to acquire an EFT-like phenotype upon the expression of EWS/ETS. Unlike what is seen for human primary fibroblasts (31), ectopic EWS/ETS expression induces an EFT-like morphological change in human MPCs, suggesting that the cell type affects susceptibility to the events following EWS/ETS expression. In murine MPCs, retrovirally transduced EWS/FLI1 has been reported to induce the expression of CD99, a most useful marker for EFT, though the results are controversial (6, 45). However, our direct evidence obtained with UET-13 cells clearly demonstrated that CD99 expression is induced by EWS/ETS proteins in human MPCs. Moreover, we showed that the expression of CD99 might correlate with EWS/ETS-mediated morphological change, whereas the functional role of CD99 and the correlation between CD99 expression status and EWS/ETS-mediated morphological change in the development of EFT remain unclarified.

Consistent with the morphological and immunophenotypic changes, the expression pattern of a set of genes in EWS/ETS-expressing UET-13 cells shifted to that in EFT cells (Fig. 7C). Although EWS/ETS expression enhanced the ability of UET-13 cells to invade Matrigel, it did not promote migratory ability and surface-independent growth, as assessed by migration assay and soft agar colony formation assay (data not shown). We also failed to develop EFT-like tumors by injecting EWS/ETS-inducing UET-13 cells into irradiated nude mice treated with tetracycline (data not shown). These results imply that EWS/ETS expression is not sufficient to induce the full transformation in UET-13 cells, and other genetic abnormalities not regulated by EWS/ETS could still be required for the full transformation of human MPCs into EFT cells. An identification of these genes will greatly improve our understanding of the additional genetic lesions that occur after EWS/ETS expression. The genes expressed in EFT cell lines but not in EWS/ETS-expressing UET-13 cells would be candidates for such genes.

In summary, we reported the development of an inducible EWS/ETS expression system in UET-13 cells as a model for the development of EFT in MPCs. In our system, the chimeric genes alone are sufficient to confer EFT-like phenotypes, EFT-specific gene expression pattern, and partial but not full features of malignant transformation. Further analysis using our system should elucidate the pathogenic mechanism by which EFTs develop from MPCs, especially the initiating events mediated by EWS/ETS expression. Our system should also aid in the identification of novel targets of the EWS/ETS-mediated pathway as potential anticancer targets.

ACKNOWLEDGMENTS

This work was supported in part by health and labor sciences research grants (the 3rd-Term Comprehensive 10-Year Strategy for Cancer Control [H19-010], Research on Children and Families [H18-005 and H19-003], Research on Human Genome Tailor Made, and Research on Publicly Essential Drugs and Medical Devices [H18-005[) and a grant for child health and development from the Ministry of Health, Labor and Welfare of Japan, JSPS (Kakenhi 18790263). This work was also supported by a CREST, JST grant from the Japan Health Sciences Foundation for Research on Publicly Essential Drugs and Medical Devices and the Budget for Nuclear Research of the Ministry of Education, Culture, Sports, Science and Technology, based on screening and counseling by the Atomic Energy Commission. Y. Miyagawa is an awardee of a research resident fellowship from the Foundation for Promotion of Cancer Research (Japan) for the 3rd-Term Comprehensive 10-Year Strategy for Cancer Control.

We are grateful to T. Motoyama for the NRS-1 cell line. We respectfully thank S. Yamauchi for her secretarial work and M. Itagaki for many helpful discussions and support.

REFERENCES

1. **Akagi, T.** 2004. Oncogenic transformation of human cells: shortcomings of rodent model systems. Trends Mol. Med. **10**:542–548.
2. **Ambros, I. M., P. F. Ambros, S. Strehl, H. Kovar, H. Gadner, and M. Salzer-Kuntschik.** 1991. MIC2 is a specific marker for Ewing's sarcoma and peripheral primitive neuroectodermal tumors. Evidence for a common histogenesis of Ewing's sarcoma and peripheral primitive neuroectodermal tumors from MIC2 expression and specific chromosome aberration. Cancer **67**:1886–1893.
3. **Arvand, A., and C. T. Denny.** 2001. Biology of EWS/ETS fusions in Ewing's family tumors. Oncogene **20**:5747–5754.
4. **Bertani, N., P. Malatesta, G. Volpi, P. Sonego, and R. Perris.** 2005. Neurogenic potential of human mesenchymal stem cells revisited: analysis by immunostaining, time-lapse video and microarray. J. Cell Sci. **118**:3925–3936.
5. **Bloom, E. T.** 1972. Further definition by cytotoxicity tests of cell surface antigens of human sarcomas in culture. Cancer Res. **32**:960–967.
6. **Castillero-Trejo, Y., S. Eliazer, L. Xiang, J. A. Richardson, and R. L. Ilaria, Jr.** 2005. Expression of the EWS/FLI-1 oncogene in murine primary bone-derived cells results in EWS/FLI-1-dependent, Ewing sarcoma-like tumors. Cancer Res. **65**:8698–8705.
7. **Colter, D. C., I. Sekiya, and D. J. Prockop.** 2001. Identification of a subpopulation of rapidly self-renewing and multipotential adult stem cells in colonies of human marrow stromal cells. Proc. Natl. Acad. Sci. USA **98**: 7841–7845.
8. **Conget, P. A., and J. J. Minguell.** 1999. Phenotypical and functional properties of human bone marrow mesenchymal progenitor cells. J. Cell. Physiol. **181**:67–73.
9. **Davis, S., and P. S. Meltzer.** 2006. Ewing's sarcoma: general insights from a rare model. Cancer Cell **9**:331–332.
10. **Deneen, B., and C. T. Denny.** 2001. Loss of p16 pathways stabilizes EWS/FLI1 expression and complements EWS/FLI1 mediated transformation. Oncogene **20**:6731–6741.
11. **Deneen, B., S. M. Welford, T. Ho, F. Hernandez, I. Kurland, and C. T. Denny.** 2003. PIM3 proto-oncogene kinase is a common transcriptional target of divergent EWS/ETS oncoproteins. Mol. Cell. Biol. **23**:3897–3908.
12. **Eliazer, S., J. Spencer, D. Ye, E. Olson, and R. L. Ilaria, Jr.** 2003. Alteration of mesodermal cell differentiation by EWS/FLI-1, the oncogene implicated in Ewing's sarcoma. Mol. Cell. Biol. **23**:482–492.
13. **Fujii, Y., Y. Nakagawa, T. Hongo, Y. Igarashi, Y. Naito, and M. Maeda.** 1989. Cell line of small round cell tumor originating in the chest wall: W-ES. Hum. Cell **2**:190–191. (In Japanese.)
14. **Fukuma, M., H. Okita, J. Hata, and A. Umezawa.** 2003. Upregulation of Id2, an oncogenic helix-loop-helix protein, is mediated by the chimeric EWS/ets protein in Ewing sarcoma. Oncogene **22**:1–9.
15. **Gilbert, F., G. Balaban, P. Moorhead, D. Bianchi, and H. Schlesinger.** 1982.

Abnormalities of chromosome 1p in human neuroblastoma tumors and cell lines. Cancer Genet. Cytogenet. **7**:33–42.
16. **Girish, V., and A. Vijayalakshmi.** 2004. Affordable image analysis using NIH Image/ImageJ. Indian J. Cancer **41**:47.
17. **Gonzalez, I., E. J. Andreu, A. Panizo, S. Inoges, A. Fontalba, J. L. Fernandez-Luna, M. Gaboli, L. Sierrasesumaga, S. Martin-Algarra, J. Pardo, F. Prosper, and E. de Alava.** 2004. Imatinib inhibits proliferation of Ewing tumor cells mediated by the stem cell factor/KIT receptor pathway, and sensitizes cells to vincristine and doxorubicin-induced apoptosis. Clin. Cancer Res. **10**:751–761.
18. **Hansen, M. B., S. E. Nielsen, and K. Berg.** 1989. Re-examination and further development of a precise and rapid dye method for measuring cell growth/cell kill. J. Immunol. Methods **119**:203–210.
19. **Hara, S., E. Ishii, S. Tanaka, J. Yokoyama, K. Katsumata, J. Fujimoto, and J. Hata.** 1989. A monoclonal antibody specifically reactive with Ewing's sarcoma. Br J. Cancer **60**:875–879.
20. **Hatori, M., H. Doi, M. Watanabe, H. Sasano, M. Hosaka, S. Kotajima, F. Urano, J. Hata, and S. Kokubun.** 2006. Establishment and characterization of a clonal human extraskeletal Ewing's sarcoma cell line, EES1. Tohoku J. Exp. Med. **210**:221–230.
21. **Homma, C., Y. Kaneko, K. Sekine, S. Hara, J. Hata, and M. Sakurai.** 1989. Establishment and characterization of a small round cell sarcoma cell line, SCCH-196, with t(11;22)(q24;q12). Jpn. J. Cancer Res. **80**:861–865.
22. **Hubert, R. S., I. Vivanco, E. Chen, S. Rastegar, K. Leong, S. C. Mitchell, R. Madraswala, Y. Zhou, J. Kuo, A. B. Raitano, A. Jakobovits, D. C. Saffran, and D. E. Afar.** 1999. STEAP: a prostate-specific cell-surface antigen highly expressed in human prostate tumors. Proc. Natl. Acad. Sci. USA **96**:14523–14528.
23. **Hu-Lieskovan, S., J. Zhang, L. Wu, H. Shimada, D. E. Schofield, and T. J. Triche.** 2005. EWS-FLI1 fusion protein up-regulates critical genes in neural crest development and is responsible for the observed phenotype of Ewing's family of tumors. Cancer Res. **65**:4633–4644.
24. **Im, Y. H., H. T. Kim, C. Lee, D. Poulin, S. Welford, P. H. Sorensen, C. T. Denny, and S. J. Kim.** 2000. EWS-FLI1, EWS-ERG, and EWS-ETV1 oncoproteins of Ewing tumor family all suppress transcription of transforming growth factor beta type II receptor gene. Cancer Res. **60**:1536–1540.
25. **Jones, E. A., S. E. Kinsey, A. English, R. A. Jones, L. Straszynski, D. M. Meredith, A. F. Markham, A. Jack, P. Emery, and D. McGonagle.** 2002. Isolation and characterization of bone marrow multipotential mesenchymal progenitor cells. Arthritis Rheum. **46**:3349–3360.
26. **Khoury, J. D.** 2005. Ewing sarcoma family of tumors. Adv. Anat. Pathol. **12**:212–220.
27. **Kiyokawa, N., Y. Kokai, K. Ishimoto, H. Fujita, J. Fujimoto, and J. I. Hata.** 1990. Characterization of the common acute lymphoblastic leukaemia antigen (CD10) as an activation molecule on mature human B cells. Clin. Exp. Immunol. **79**:322–327.
28. **Konemann, S., T. Bolling, A. Schuck, J. Malath, A. Kolkmeyer, K. Horn, D. Riesenbeck, S. Hesselmann, R. Diallo, J. Vormoor, and N. A. Willich.** 2003. Effect of radiation on Ewing tumour subpopulations characterized on a single-cell level: intracellular cytokine, immunophenotypic, DNA and apoptotic profile. Int. J. Radiat. Biol. **79**:181–192.
29. **Kovar, H., and A. Bernard.** 2006. CD99-positive "Ewing's sarcoma" from mouse bone marrow-derived mesenchymal progenitor cells? Cancer Res. **66**:9786.
30. **Kovar, H., M. Dworzak, S. Strehl, E. Schnell, I. M. Ambros, P. F. Ambros, and H. Gadner.** 1990. Overexpression of the pseudoautosomal gene MIC2 in Ewing's sarcoma and peripheral primitive neuroectodermal tumor. Oncogene **5**:1067–1070.
31. **Lessnick, S. L., C. S. Dacwag, and T. R. Golub.** 2002. The Ewing's sarcoma oncoprotein EWS/FLI induces a p53-dependent growth arrest in primary human fibroblasts. Cancer Cell **1**:393–401.
32. **Lin, P. P., R. I. Brody, A. C. Hamelin, J. E. Bradner, J. H. Healey, and M. Ladanyi.** 1999. Differential transactivation by alternative EWS-FLI1 fusion proteins correlates with clinical heterogeneity in Ewing's sarcoma. Cancer Res. **59**:1428–1432.
33. **Lipinski, M., K. Braham, I. Philip, J. Wiels, T. Philip, C. Goridis, G. M. Lenoir, and T. Tursz.** 1987. Neuroectoderm-associated antigens on Ewing's sarcoma cell lines. Cancer Res. **47**:183–187.
34. **Lochter, A., A. Srebrow, C. J. Sympson, N. Terracio, Z. Werb, and M. J. Bissell.** 1997. Misregulation of stromelysin-1 expression in mouse mammary tumor cells accompanies acquisition of stromelysin-1-dependent invasive properties. J. Biol. Chem. **272**:5007–5015.
35. **May, W. A., A. Arvand, A. D. Thompson, B. S. Braun, M. Wright, and C. T. Denny.** 1997. EWS/FLI1-induced manic fringe renders NIH 3T3 cells tumorigenic. Nat. Genet. **17**:495–497.
36. **May, W. A., S. L. Lessnick, B. S. Braun, M. Klemsz, B. C. Lewis, L. B. Lunsford, R. Hromas, and C. T. Denny.** 1993. The Ewing's sarcoma EWS/FLI-1 fusion gene encodes a more potent transcriptional activator and is a more powerful transforming gene than FLI-1. Mol. Cell. Biol. **13**:7393–7398.
37. **Miyagawa, Y., J. M. Lee, T. Maeda, K. Koga, Y. Kawaguchi, and T. Kusakabe.** 2005. Differential expression of a Bombyx mori AHA1 homologue during spermatogenesis. Insect Mol. Biol. **14**:245–253.
38. **Mori, T., T. Kiyono, H. Imabayashi, Y. Takeda, K. Tsuchiya, S. Miyoshi, H. Makino, K. Matsumoto, H. Saito, S. Ogawa, M. Sakamoto, J. Hata, and A. Umezawa.** 2005. Combination of hTERT and bmi-1, E6, or E7 induces prolongation of the life span of bone marrow stromal cells from an elderly donor without affecting their neurogenic potential. Mol. Cell. Biol. **25**:5183–5195.
39. **Nishimori, H., Y. Sasaki, K. Yoshida, H. Irifune, H. Zembutsu, T. Tanaka, T. Aoyama, T. Hosaka, S. Kawaguchi, T. Wada, J. Hata, J. Toguchida, Y. Nakamura, and T. Tokino.** 2002. The Id2 gene is a novel target of transcriptional activation by EWS-ETS fusion proteins in Ewing family tumors. Oncogene **21**:8302–8309.
40. **Ogose, A., T. Motoyama, T. Hotta, and H. Watanabe.** 1995. In vitro differentiation and proliferation in a newly established human rhabdomyosarcoma cell line. Virchows Arch. **426**:385–391.
41. **Prieur, A., F. Tirode, P. Cohen, and O. Delattre.** 2004. EWS/FLI-1 silencing and gene profiling of Ewing cells reveal downstream oncogenic pathways and a crucial role for repression of insulin-like growth factor binding protein 3. Mol. Cell. Biol. **24**:7275–7283.
42. **Quirici, N., D. Soligo, P. Bossolasco, F. Servida, C. Lumini, and G. L. Deliliers.** 2002. Isolation of bone marrow mesenchymal stem cells by anti-nerve growth factor receptor antibodies. Exp. Hematol. **30**:783–791.
43. **Reyes, M., T. Lund, T. Lenvik, D. Aguiar, L. Koodie, and C. M. Verfaillie.** 2001. Purification and ex vivo expansion of postnatal human marrow mesodermal progenitor cells. Blood **98**:2615–2625.
44. **Reyes, M., and C. M. Verfaillie.** 2001. Characterization of multipotent adult progenitor cells, a subpopulation of mesenchymal stem cells. Ann. N. Y. Acad. Sci. **938**:231–235.
45. **Riggi, N., L. Cironi, P. Provero, M. L. Suva, K. Kaloulis, C. Garcia-Echeverria, F. Hoffmann, A. Trumpp, and I. Stamenkovic.** 2005. Development of Ewing's sarcoma from primary bone marrow-derived mesenchymal progenitor cells. Cancer Res. **65**:11459–11468.
46. **Riggi, N., M. L. Suva, and I. Stamenkovic.** 2006. Ewing's sarcoma-like tumors originate from EWS-FLI-1-expressing mesenchymal progenitor cells. Cancer Res. **66**:9786.
47. **Sekiguchi, M., T. Oota, K. Sakakibara, N. Inui, and G. Fujii.** 1979. Establishment and characterization of a human neuroblastoma cell line in tissue culture. Jpn. J. Exp. Med. **49**:67–83.
48. **Smith, R., L. A. Owen, D. J. Trem, J. S. Wong, J. S. Whangbo, T. R. Golub, and S. L. Lessnick.** 2006. Expression profiling of EWS/FLI identifies NKX2.2 as a critical target gene in Ewing's sarcoma. Cancer Cell **9**:405–416.
49. **Staege, M. S., C. Hutter, I. Neumann, S. Foja, U. E. Hattenhorst, G. Hansen, D. Afar, and S. E. Burdach.** 2004. DNA microarrays reveal relationship of Ewing family tumors to both endothelial and fetal neural crest-derived cells and define novel targets. Cancer Res. **64**:8213–8221.
50. **Takeda, Y., T. Mori, H. Imabayashi, T. Kiyono, S. Gojo, S. Miyoshi, N. Hida, M. Ita, K. Segawa, S. Ogawa, M. Sakamoto, S. Nakamura, and A. Umezawa.** 2004. Can the life span of human marrow stromal cells be prolonged by bmi-1, E6, E7, and/or telomerase without affecting cardiomyogenic differentiation? J. Gene Med. **6**:833–845.
51. **Tondreau, T., N. Meuleman, A. Delforge, M. Dejeneffe, R. Leroy, M. Massy, C. Mortier, D. Bron, and L. Lagneaux.** 2005. Mesenchymal stem cells derived from CD133-positive cells in mobilized peripheral blood and cord blood: proliferation, Oct4 expression, and plasticity. Stem Cells **23**:1105–1112.
52. **Torchia, E. C., S. Jaishankar, and S. J. Baker.** 2003. Ewing tumor fusion proteins block the differentiation of pluripotent marrow stromal cells. Cancer Res. **63**:3464–3468.
53. **Woodbury, D., E. J. Schwarz, D. J. Prockop, and I. B. Black.** 2000. Adult rat and human bone marrow stromal cells differentiate into neurons. J. Neurosci. Res. **61**:364–370.

MOLECULAR AND CELLULAR BIOLOGY, June 2008, p. 3882
0270-7306/08/$08.00+0 doi:10.1128/MCB.00557-08

Vol. 28, No. 11

ERRATUM

Inducible Expression of Chimeric EWS/ETS Proteins Confers Ewing's Family Tumor-Like Phenotypes to Human Mesenchymal Progenitor Cells

Yoshitaka Miyagawa, Hajime Okita, Hideki Nakaijima, Yasuomi Horiuchi, Ban Sato, Tomoko Taguchi, Masashi Toyoda, Yohko U. Katagiri, Junichiro Fujimoto, Jun-ichi Hata, Akihiro Umezawa, and Nobutaka Kiyokawa

Department of Developmental Biology, National Research Institute for Child Health and Development, 2-10-1, Okura, Setagaya-ku, Tokyo 157-8535, Japan; National Research Institute for Child Health and Development, 2-10-1, Okura, Setagaya-ku, Tokyo 157-8535, Japan; and Department of Reproductive Biology, National Research Institute for Child Health and Development, 2-10-1, Okura, Setagaya-ku, Tokyo 157-8535, Japan

Volume 28, no. 7, p. 2125–2137, 2008. Page 2131: The boxheads for Table 2 should appear as shown below.

MPC status[a]	CD marker	Result for[b]: UET-13	UET-13R Tet⁻	UET-13R Tet⁺	UET-13TR-EWS/FLI Tet	UET-13TR-EWS/FLI Tet⁺	UET-13TR-EWS/ERG Tet⁻	UET-13TR-EWS/ERG Tet⁺	RD-ES	SK-ES1	EFT status[c]

STEM CELLS
TISSUE-SPECIFIC STEM CELLS

Novel Cardiac Precursor-Like Cells from Human Menstrual Blood-Derived Mesenchymal Cells

NAOKO HIDA,[a,b,c] NOBUHIRO NISHIYAMA,[a,c] SHUNICHIRO MIYOSHI,[a,d] SHINICHIRO KIRA,[a] KAORU SEGAWA,[e] TARO UYAMA,[b] TAISUKE MORI,[c] KENJI MIYADO,[b] YUKINORI IKEGAMI,[a,b] CHANGHAO CUI,[b] TOHRU KIYONO,[f] SATORU KYO,[g] TATSUYA SHIMIZU,[h] TERUO OKANO,[h] MICHIIE SAKAMOTO,[c] SATOSHI OGAWA,[a] AKIHIRO UMEZAWA[b]

[a]Department of Cardiology, Keio University School of Medicine, Tokyo, Japan; [b]Department of Reproductive Biology and Pathology, National Research Institute for Child Health and Development, Tokyo, Japan; [c]Department of Pathology, Keio University School of Medicine, Tokyo, Japan; [d]Institute for Advanced Cardiac Therapeutics, Keio University School of Medicine, Tokyo, Japan; [e]Department of Microbiology and Immunology, Keio University School of Medicine, Tokyo, Japan; [f]Virology Division, National Cancer Center Research Institute, Tokyo, Japan; [g]Department of Obstetrics and Gynecology, Kanazawa University, School of Medicine, Kanazawa, Japan; [h]Institute of Advanced Biomedical Engineering and Science, Tokyo Women's Medical University, Tokyo, Japan

Key Words. Cardiomyogenesis human mesenchymal stem cell • Menstrual blood endometrial gland • Cell sheet technology cardiac precursors

ABSTRACT

Stem cell therapy can help repair damaged heart tissue. Yet many of the suitable cells currently identified for human use are difficult to obtain and involve invasive procedures. In our search for novel stem cells with a higher cardiomyogenic potential than those available from bone marrow, we discovered that potent cardiac precursor-like cells can be harvested from human menstrual blood. This represents a new, noninvasive, and potent source of cardiac stem cell therapeutic material. We demonstrate that menstrual blood-derived mesenchymal cells (MMCs) began beating spontaneously after induction, exhibiting cardiomyocyte-specific action potentials. Cardiac troponin-I-positive cardiomyocytes accounted for 27%–32% of the MMCs in vitro. The MMCs proliferated, on average, 28 generations without affecting cardiomyogenic transdifferentiation ability, and expressed mRNA of GATA-4 before cardiomyogenic induction. Hypothesizing that the majority of cardiomyogenic cells in MMCs originated from detached uterine endometrial glands, we established monoclonal endometrial gland-derived mesenchymal cells (EMCs), 76%–97% of which transdifferentiated into cardiac cells in vitro. Both EMCs and MMCs were positive for CD29, CD105 and negative for CD34, CD45. EMCs engrafted onto a recipient's heart using a novel 3-dimensional EMC cell sheet manipulation transdifferentiated into cardiac tissue layer in vivo. Transplanted MMCs also significantly restored impaired cardiac function, decreasing the myocardial infarction (MI) area in the nude rat model, with tissue of MMC-derived cardiomyocytes observed in the MI area in vivo. Thus, MMCs appear to be a potential novel, easily accessible source of material for cardiac stem cell-based therapy. STEM CELLS *2008;26:1695–1704*

Disclosure of potential conflicts of interest is found at the end of this article.

INTRODUCTION

Marrow-derived mesenchymal stem cells (MSCs) are a potential cellular source for stem cell-based therapy, since they have the ability to differentiate into cardiomyocytes [1, 2], use of MSCs presents no ethical problems, and autologous MSCs have been injected into ischemic hearts clinically [3]. Direct injection of MSCs into the heart has been shown to be feasible in vivo [4–7], but with limited effect. The reason for this may be the extremely low rate of cardiomyogenesis exhibited by marrow-derived MSCs [2], with cardiac function improvement due to grafted MSC-induced neovascularization [7, 8] and an antiapoptotic

Author contributions: N.H.: conception and design, collection and assembly of data, data analysis and interpretation, final approval of manuscript; N.N.: conception and design, collection and assembly of data, data analysis and interpretation, manuscript writing, final approval of manuscript; S.M.: conception and design, administrative support, collection and assembly of data, data analysis and interpretation, manuscript writing, final approval of manuscript; S. Kira and Y.I.: collection and assembly of data, final approval of manuscript; K.S., C.C., T.K., S. Kyo, and T.S.: provision of study material, final approval of manuscript; T.U.: provision of study material, collection and assembly of data, final approval of manuscript; T.M.: collection and assembly of data, data analysis and interpretation, final approval of manuscript; K.M.: collection and assembly of data, final approval of manuscript; T.O.: administrative support, provision of study material, final approval of manuscript; M.S.: administrative support, final approval of manuscript; S.O.: financial support, administrative support, final approval of manuscript; A.U.: financial support, administrative support, manuscript writing, final approval of manuscript.

Correspondence: Shunichiro Miyoshi M.D., Ph.D., Keio University School of Medicine, 35-Shinanomachi, Shinjuku-ku, Tokyo, 160-8582 Japan. Telephone: +81-3-3353-1211 (ext 62310); Fax: +81-3-3353-2502; e-mail: smiyoshi@cpnet.med.keio.ac.jp Received October 2, 2007; accepted for publication April 6, 2008; first published online in STEM CELLS *EXPRESS* April 17, 2008. 1066-5099/2008/$30.00/0 doi: 10.1634/stemcells.2007-0826

effect on infarcted cardiomyocytes [9, 10]. To further improve prospects of restoring cardiac function, a search was initiated for another source of cells having high cardiomyogenic potential.

Our previous study showed that umbilical cord blood-derived mesenchymal stem cells (UCBMSCs) [11] and placental chorionic plate cells (PCPCs) [12] have a phenotype of mesenchymal cells and have higher cardiomyogenic differentiation ability in vitro. Since these materials are deemed medical waste and can be obtained without any ethical problems, they may be a suitable stem cell source for cardiac regenerative therapy. But the population of UCBMSCs in umbilical cord blood is scant [13] and there is also a problem in establishing PCPCs, since placental tissue contains a lot of maternal decidua-derived mesenchymal cells that could contaminate PCPCs. Therefore, it is difficult to obtain enough of these cells without using a limiting dilution method and/or massive ex vivo propagation, which may cause instability of the genome [14]. Consequently, material that contains a large amount of mesenchymal cells during the first few passages should be a highly suitable source of stem cells.

A previous paper suggests that endometrium contains an MSC-like population [15] and menstrual blood-derived mesenchymal (MMCs) cells have a pluripotent differentiation ability in vitro [16]. The data presented here demonstrate that human menstrual blood-derived mesenchymal cells and uterine endometrial gland-derived mesenchymal cells (EMCs) have a strong potential for cardiomyogenic transdifferentiation in vitro and in vivo. Moreover, large amounts of MMCs could be obtained from the first passage of menstrual blood culture, and MMCs have been shown to restore impaired cardiac function through marked cardiomyogenesis in vivo.

MATERIALS AND METHODS

Isolation of MMCs and EMCs

After informed consent was obtained, mesenchymal cells from approximately 10 ml of menstrual blood of six women (20–30 years old) were collected on the first day of menstruation. The samples were suspended in Dulbecco's modified Eagle's medium (DMEM) high glucose supplemented with 10% FBS, and split into two 10-cm dishes. The estimated adherent cell number at the start of culture was approximately 1×10^7. The growth curve and phase-contrast microscopic view are shown in supplemental online Fig. 1. The results for MMCs obtained from six women were the same. A human endometrial tissue sample was also taken from a 52-year-old woman undergoing hysterectomy [17]. Individual endometrial glands were isolated under a microscope and then seeded. After the retroviral transfection of HPV16E6, E7, and hTERT [2], endometrial cell strains were generated by the limiting dilution method. Two strains exhibiting rapid cell division cycles were designated EMC100 and EMC214 (Fig. 3B and 3D, respectively). EMC100 and EMC214 showed adherent spindle shape morphology that proliferated for more than 250 population doublings without changing cardiomyogenic differentiation ability.

Isolation of Marrow-Derived Mesenchymal Stem Cells

Bone marrow-derived mesenchymal stem cells (BMMSCs) were obtained from a 41-year-old male as described previously [2].

Coculture with Murine Fetal Cardiomyocytes

MMCs, EMCs, and BMMSCs were infected with enhanced green fluorescent protein (EGFP) expressing adenovirus [2]. Fetal cardiomyocytes were obtained from hearts of day-17 mouse fetuses, as previously described [2]. The isolated cardiomyocytes were replated at $5 \times 10^4/cm^2$ on top of a floating athelocollagen membrane (CM-6, 40-μm thickness; Koken, Tokyo, http://www.kokenmpc.co.jp/english/products/collagen/cell_culture/cm-6_24/index.html) that is permeable for only small molecules (less than 5,000 MW). The next day, the athelocollagen membrane was plated upside down on the culture dish. Harvested EGFP-labeled MMCs and EMCs were then seeded upon the athelocollagen surface (bottom surface) at $7 \times 10^3/cm^2$ (Fig. 1M). In several experiments (Figs. 1G–1L, 2, 3E, 3H, 3K–3M, 4, supplemental online Fig. 2, examination of chromosome chimeras), we did not use the athelocollagen membrane for the coculture system.

Immunocytochemistry and Immunohistochemistry

A laser confocal microscope (FV1000; Olympus, Tokyo, http://www.olympus-global.com) was used for immunocytochemical analysis. Samples were stained with mouse monoclonal anti-cardiac troponin-I antibody (4T21 Lot 98/10-T21-C2; HyTest, Euro, Finland, http://www.hytest.fi/) or with mouse monoclonal anti-sarcomeric α-actinin antibody (Sigma-Aldrich, St. Louis, http://www.sigmaaldrich.com), or anti-connexin 43 antibody (Sigma-Aldrich) diluted 1:300 overnight at 4°C, then stained with TRITC-conjugated anti-mouse antibody (Sigma-Aldrich), TRITC-conjugated anti-rabbit antibody (Sigma-Aldrich), and Cy5-conjugated anti-mouse IgG (Chemicon, Temecula, CA, http://www.chemicon.com) diluted 1:100, containing 4′-6-diamidino-2-phenylindole (DAPI; Wako Chemical, Osaka, Japan, http://www.wako-chem.co.jp/english) at 1:300 for 30 minutes at 25°C–28°C. See also supplemental online data 1 for detail of method.

Functional Analysis

The method of action potential (AP) recording was as previously described [2] but with slight modification. A fluorescence inverted microscope (IX-70; Olympus) was used for AP recording. The microscope was equipped with a recording chamber and a noiseless heating plate (Microwarm Plate; Kitazato Supply, Fujinomiya, Shizuoka, Japan, http://www.kitazato-supply.com). A 10-mM volume of HEPES (Sigma-Aldrich) was added to the culture medium to stabilize the pH of the perfusate at 7.5. Standard glass microelectrodes having a direct current resistance of 15–25 MΩ when filled with pipette solution were used. Alexa 568 compound was dissolved to a concentration of 0.5 mM in 2 M of KCl solution in order to completely dissolve the Alexa 568 in the pipette solution. The electrodes were positioned with a motor-driven micromanipulator (PCS-5000; Burleigh Instrument, Inc., New York) under optical control. Spontaneously beating EGFP-positive cells were selected as targets, and after the APs of the target cells had been recorded, the dye was injected by iontophoresis (−7 nA for 10–20 seconds). The extent of dye transfer was monitored under a fluorescence microscope, and digital images were recorded with a digital photo camera (EOS-digital; Canon, Tokyo, http://www.canon.com) mounted on the microscope. The recording pipette was connected to a patch-clamp amplifier (MEZ-8300; Nihon Kohden, Tokyo, http://www.nihonkohden.com). The amplified signal was filtered with a 4-pole Bessel filter (NF-3625; NF electronic instrument; NF Corp., Tokyo, http://www.nfcorp.co.jp/english/index.html) set at 2 kHz, then digitized with an A/D converter with a sampling frequency of 10 kHz (Digidata 1,322A; Molecular Devices Corp., Union City, CA, http://www.moleculardevices.com). Pacemaker potential was defined by the slowly depolarizing membrane potential at phase IV of the AP.

Alexa 568 was injected into cells via recording microelectrodes to stain the cells and confirm that the AP was generated by EGFP-positive cells (Fig. 1G–1I, 3E, 3H). Since the dye did not diffuse into the EGFP-negative murine cardiomyocytes, there were no tight cell-to-cell heterologous connections (i.e., gap junctions), at least in the in vitro condition. In some experiments, Alexa 568 diffused into the EGFP-positive satellite EMCs and MMCs, suggesting that a homologous cell-to-cell connection had been established at least 1 week after cocultivation. The measured parameters of the APs were averaged and are shown in Figure 1K.

The fluorescent image of the beating MMCs and EMCs was monitored using a CCD camera (Ikegami Tsushin Co., Ltd, http://www.ikegami.co.jp) and was stored using digital video. The video images (National Television Standards Committee format, 29.97 frame/second) of contraction of EMCs and MMCs were stored in a personal computer as MPEG-2 format files, then analyzed later.

Both edges of the EGFP-positive EMCs and MMCs along the line (Figs. 1L, 3K) were automatically detected, and the distance between both edges was measured from each video frame using an image edge-detection program using Igor Pro 4 (Wavemetrics Inc., Lake Oswego, OR) [11].

Calculation of Induction Rate

The MMCs and EMCs were exposed to 3 μM 5-azacytidine (5-azaC; Sigma-Aldrich) for 24 hours to induce cell differentiation, or were left untreated. The 5-azaC-treated and nontreated MMCs or EMCs, cultivated with or without murine fetal cardiomyocytes, were enzymatically dissociated and stained, then observed by confocal laser microscope (supplemental online data 2 for detail of method). The cardiomyogenic induction rate (average of 10 separate experiments) was calculated as the fraction of cardiac troponin-I-positive cells in the EGFP-positive cells.

Examination of Chromosomes of MMCs or EMCs and Murine Cell Chimeras

To rule out cell fusion-dependent cardiomyogenesis, chromosomes from MMCs or EMCs cocultivated without separation by the athelocollagen membrane from murine cardiomyocytes for 1 week were stained using a human chromosome-specific probe and a mouse chromosome-specific probe (Chromosome Science Labo, Hokkaido, Japan, http://www.chromoscience.jp/en/probe/page01/page01e.html) and spectral karyotyping with fluorescent in situ hybridization chromosome painting technique (Applied Spectral Imaging, Vista, CA, http://www.spectral-imaging.com), according to the manufacturer's protocol.

RNA Extraction and RT-PCR

Reverse transcriptase polymerase chain reaction (RT-PCR) was done as described previously [2]. Primers for the following genes were used: cardiac transcription factors—Csx/Nkx-2.5 and GATA4; cardiac hormones—atrial natriuretic peptide and brain natriuretic peptide; cardiac structural proteins—cardiac troponin I, cardiac troponin T, myosin light chain-2a, myosin light chain-2v, and cardiac-actin; and ion channel—cyclic nucleotide-gated potassium channel 2 (supplemental online Table 1). The internal control was 18S rRNA. PCR primers were prepared such that they would amplify the human but not the mouse genes.

Flow Cytometric Analysis

The cells were analyzed using an EPICS ALTRA analyzer (Beckman Coulter, Fullerton, CA, http://www.beckmancoulter.com). Antibodies (anti-human CD10, CD13, CD14, CD24, CD29, CD31, CD34, CD44, CD45, CD54, CD55, CD59, CD71, CD73, CDw90, CD105, CD106, CD117, CD133, CD140a, CD166, CD309, HLA-ABC, and HLA-DR) [12] were purchased from Beckman Coulter, Immunotech (Luminy, France, http://www.beckmancoulter.com/products/pr_immunology.asp), Cytotech (Hellebaek, Denmark, http://www.cytotech.dk/index.html), Santa Cruz Biotechnology Inc. (Santa Cruz, CA, http://www.scbt.com), RDI (Research Diagnostics, Inc., Concord, MA, http://www.researchd.com), and Pharmingen Pharmaceutical, Inc. (San Diego, http://www.bdbiosciences.com/index_us.shtml).

In Vivo Cardiomyogenic Differentiation of EMCs

EGFP-labeled EMC tissue graft, made by a novel 3-dimensional cell sheet manipulation, was transplanted into male F344 nude rats (Clea, Tokyo, http://www.clea-japan.com/) (8 weeks of age). EMC100s and EMC214s (2×10^5/cm^2) were plated onto fibrin polymer-coated culture dishes. Four days after plating, EMCs were detached as previously described [18], and transplanted onto the surface of the recipient heart (Fig. 5A) [19]. At 2 weeks after transplantation, immunohistochemical analysis was performed. EGFP-labeled EMC tissue graft on the fibrin polymer-coated culture dish did not show cardiomyogenic differentiation in vitro.

MMC Transplantation in Myocardial Infarction Model In Vivo

Recipient male F344 nude rats (Clea) (6 weeks of age) were anesthetized with 2% isoflurane gas. After left thoracotomy, the left ventricle was exposed and left anterior coronary artery was ligated by 6–0 silk suture. The complete occlusion of the coronary artery was confirmed by the cyanotic color and dyskinetic motion of the left ventricular anterior wall. In some rats, we did not ligate the coronary artery (Sham). The chest was closed and animals survived for 2 weeks to create complete myocardial infarction.

Two weeks after the first operation, rats with myocardial infarction were randomized for the control myocardial infarction (MI) group, the MI+BMMSC group, and the MI+MMC group, and were blinded immediately before the cell injection. Echocardiograms were performed on the anesthetized (2% isoflurane) rats. Data were collected three times and averaged. Immediately before transplantation, $\sim 1–2 \times 10^6$ of EGFP-positive MMC or BMMSC suspension was drawn up into a 50-μl Hamilton syringe (Hamilton Co., Reno, NV, http://www.hamiltoncompany.com/main_usa.asp) with a 31-gauge needle. A 10-μl portion of the cell suspension was injected into the center and margin of the infarcted myocardium (MI+MMC, Fig. 7A). In the control MI group, culture medium or $\sim 1–2 \times 10^6$ of murine cardiac fibroblast was injected. Immediately before cell transplantation, 2-dimensional and M-mode echocardiographic (8.5 MHz linear transducer, EnVisor C; Phillips Medical System, Andover, MA, http://www.medical.philips.com/index.html) images were obtained to assess left ventricular (LV) end-diastolic dimension and LV end-systolic dimension at the mid-papillary muscle level.

Two weeks after the transplantation, a similar echocardiogram was performed again; then after opening the abdomen, a blood sample was drawn from the abdominal great vein; then the left diaphragm was dissected to insert a 22-gauge manometer line into the left ventricle, which was connected to the transducer (model TP-400T; Nihon Kohden) to monitor left ventricular pressure. The electrocardiogram and measured pressure were digitized by PowerLabo (ADInstruments, Milford, MA, http://www.adinstruments.com) at the sample frequency of 10 KHz and stored in a personal computer (Macintosh iBook G4; Apple, Cupertino, CA, http://www.apple.com).

Tissue samples were obtained by fixing and slicing along the short axis of the left ventricle, for every 1-mm depth of the ventricle. After Masson's trichrome staining, digital images of samples were collected using a light microscope (IX-70; Olympus). The images were digitized and analyzed using an Igor Pro 4 (Wavemetrics Inc.). The pixel area of blue color (fibrosis area) was defined as the infarcted area, and the pixel area of red color was defined as "survived" myocardium. The data on each pixel area from each slice were collated and the percentage fibrosis area was calculated as follows: % Fibrosis = 100 × (Pixel area of blue color)/(Pixel area of blue color and red color).

Statistical Analysis

All data are shown as the mean value ± SE. The difference among mean values was determined with analysis of variance. The posthoc test (Bonferroni) was used when three or more groups were compared. Student's t test was used when two values were compared. Statistical significance was set at $p < .05$.

RESULTS

Cardiomyogenic Transdifferentiation of MMCs

To exclude cell fusion-dependent cardiomyogenesis [20], EGFP-labeled MMCs were cocultured in the same dish with mouse cardiomyocytes, separated by a 40-μm high-density athelocollagen membrane (Fig. 1M). The two cell types were never in direct contact. On day 5 after cocultivation commenced, approximately half of the MMCs were beating strongly in a synchronized manner (supplemental online Video 1). Im-

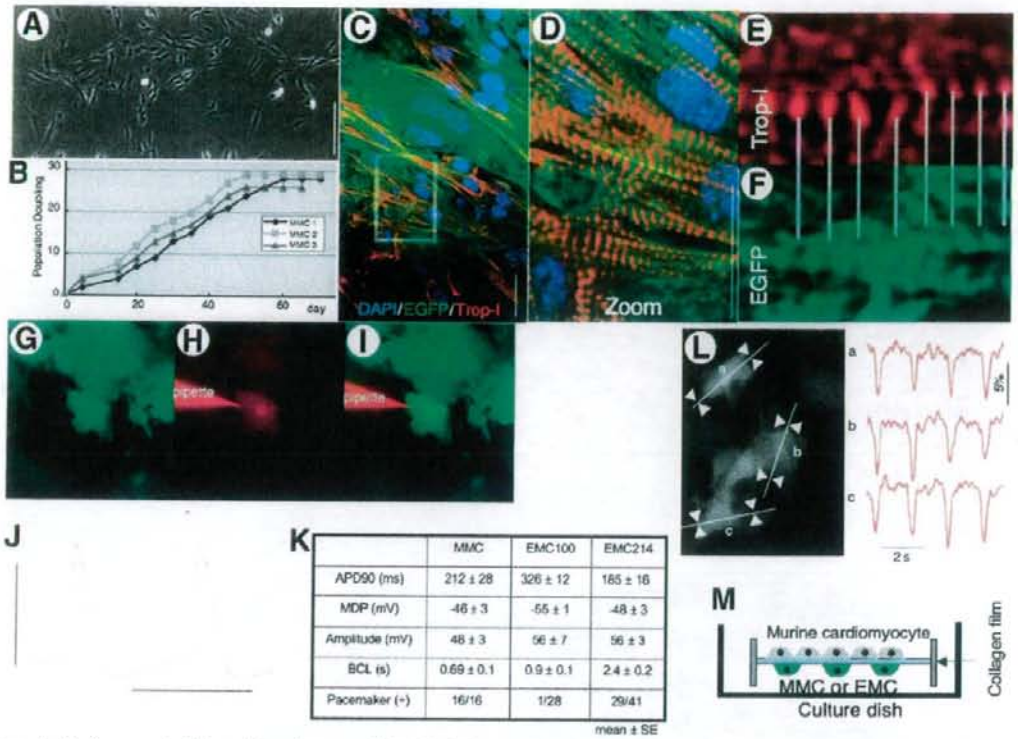

	MMC	EMC100	EMC214
APD90 (ms)	212 ± 28	326 ± 12	185 ± 16
MDP (mV)	-46 ± 3	-55 ± 1	-48 ± 3
Amplitude (mV)	48 ± 3	56 ± 7	56 ± 3
BCL (s)	0.69 ± 0.1	0.9 ± 0.1	2.4 ± 0.2
Pacemaker (+)	16/16	1/28	29/41

mean ± SE

Figure 1. Cardiomyogenic differentiation of menstrual blood-derived mesenchymal cells (MMCs) in vitro. **(A):** Phase-contrast microscopic view of MMC (bar denotes 100 μm), regarded as being PD1, or day 2. **(B):** The representative growth curves of MMCs as a function of time after the culture. The growth curves from all three donors are linear over at least 25 population doublings. **(C–F):** Laser confocal microscopic view of immunocytochemistry of differentiated MMCs with anti-cardiac troponin-I (Trop-I) antibody. Enhanced green fluorescent protein (EGFP)-positive (green) human MMCs expressed Trop-I (red). Scale bar denotes 20 μm. **(D):** Expansion of area within the white box in **(C)**. Clear striation pattern of Trop-I is observed. Trop-I and EGFP images along the yellow line are shown in **(E, F)**. **(E, F):** Trop-I and EGFP staining was observed alternately in striated manner, suggesting Trop-I is expressed in the EGFP-positive cell. **(G–I):** EGFP-labeled MMCs were injected with Alexa 568 solution (red) through a microelectrode to confirm that the recorded signal was obtained from MMCs. **(J):** Representative action potential traces are shown (horizontal line denotes 500 ms). The vertical line denotes 50 mV, and dotted horizontal line denotes 0 mV. **(K):** Action potential parameters. **(L):** A representative still image (left panel) and detected fractional shortening (% FS) along the white line obtained from sites a, b, and c are shown in right panel. **(M):** Experimental schema. Abbreviations: ADP, action potential duration; BCL, basic cycle length; DAPI, 4′-6-diamidino-2-phenylindole; MDP, maximum diastolic potential.

munocytochemistry revealed that the MMCs were stained positive by the anti-cardiac troponin-I antibody (Fig. 1C–1E). Clear striations of red fluorescence of troponin-I in the differentiated MMCs (Fig. 1D, 1E) were observed. Troponin-I and EGFP staining appeared alternately in a striated manner, suggesting troponin-I expressed in the EGFP-positive cell (Fig. 1E, 1F). Clear striations were observed with red fluorescence of α-actinin in the differentiated MMCs (Fig. 2B) and diffuse dot-like staining pattern of connexin 43 around the margin of each EGFP-positive cardiomyocyte (Fig. 2C–2F), suggesting that these human transdifferentiated cardiomyocytes have tight electrical coupling with each other. APs were recorded from spontaneously beating MMCs. The APs obtained from MMCs showed clear cardiomyocyte-specific sustained plateaus and slowly depolarizing resting membrane potentials—so-called "pacemaker potentials" (Fig. 1J, 1K)—and were, therefore, determined to be APs of cardiomyocytes, not of smooth muscle cells, nerve cells, or skeletal muscle cells. The fractional shortening (% FS) of the MMCs was analyzed (Fig. 1L) using a cell edge detection program. The EGFP-positive cells contracted simultaneously within the whole visual field. The % FS was 5.9 ± 0.5% (n = 19).

The percentage of cardiac troponin-I-positive cells was calculated to determine the cardiomyogenic transdifferentiation rate. Whereas MMCs without cocultivation did not show any troponin-I expression (supplemental online Figs. 1A–1D, 2A, 2B), 27%–32% of MMCs became positive for cardiac troponin-I antibody as a result of the cocultivation (Figs. 1C–1F, 4A, supplemental online Fig. 2C, 2D). A cytosine analog, 5-azaC, has a remarkable effect on cell transdifferentiation and has been shown to induce transdifferentiation BMMSCs into cardiomyocytes in mice by nonspecific demethylation of the genome [1]. Cardiomyogenic transdifferentiation was observed in the cocultivated MMCs without any 5-azaC pretreatment, meaning that 5-azaC was not essential for cardiomyogenic transdifferentiation. Nuclear fusion between the cocultivated MMCs and murine cardiomyocytes without separation of the athelocollagen membrane was observed in only 0.16% (3/1846).

Cardiomyogenic Transdifferentiation of EMCs

We hypothesized that the origin of cardiomyogenic cells in the MMCs was the endometrial gland, since MMCs have a high content of detached endometrial glands, whereas circu-

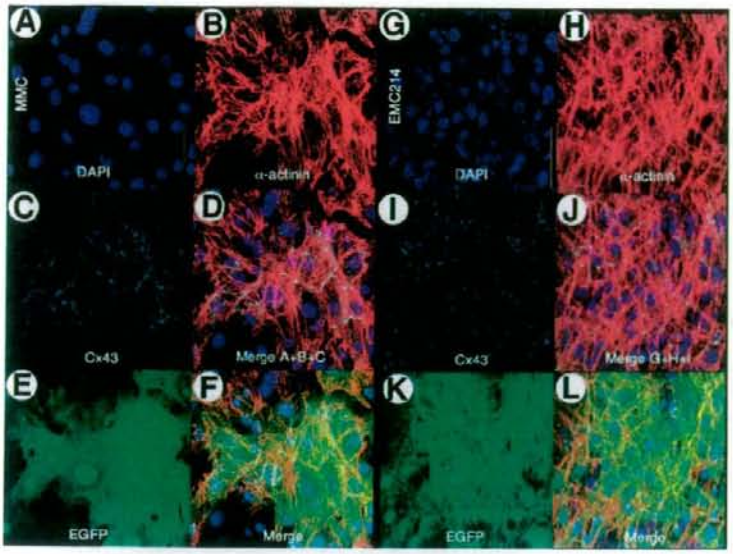

Figure 2. Immunocytochemical analysis of menstrual blood-derived mesenchymal cells (MMCs) and EMC214s stained with anti-sarcomeric α-actinin and connexin 43. **(A–L):** Laser confocal microscopic view of immunocytochemistry of differentiated MMCs and EMC214s with anti-sarcomeric α-actinin (α-actinin) and connexin 43 (Cx43) antibody. **(A–F, G–L):** Enhanced green fluorescent protein (EGFP)-positive **(E, K**; green) human MMCs and EMC214s express α-actinin **(B, H**; red) and Cx43 **(C, I**; cyan). Nuclei are stained with 4′-6-diamidino-2-phenylindole (DAPI) **(A, G**; blue). Clear striation patterns of α-actinin and diffuse Cx43 dot-like staining around the margin of the MMCs and EMC214s were observed. Scale bars in the figure denote 50 μm.

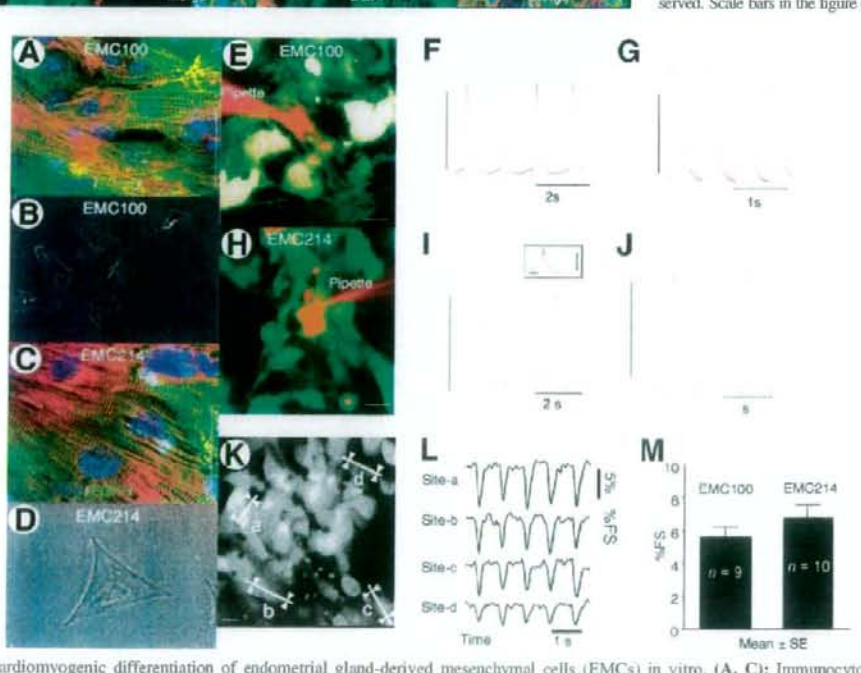

Figure 3. Cardiomyogenic differentiation of endometrial gland-derived mesenchymal cells (EMCs) in vitro. **(A, C):** Immunocytochemistry of differentiated EMC100s **(A)** and EMC214s **(C)** with anti-cardiac troponin-I (Trop-I) antibody. The cells were stained with 4′-6-diamidino-2-phenylindole (DAPI; blue), and anti-cardiac troponin-I antibody (red). Enhanced green fluorescent protein (EGFP)-positive (green) human EMCs expressed Trop-I (red). Please note clear striation staining pattern of Trop-I **(A, C)** in EMCs. Scale bar denotes 20 μm. **(B, D):** Phase-contrast images of EMC100s **(B)** and EMC214s **(D)** before the cardiomyogenic induction. **(E, H):** EGFP-labeled EMC100s and EMC214s (green) were injected with Alexa 568 solution (red) through a microelectrode **(E, H)**, and a recorded signal was obtained from the cells. Representative action potential traces are shown **(F, G**: EMC100; **I, J**: EMC214). Action potential of E is expanded in the inset (the vertical line denotes 100 ms). The vertical line denotes 50 mV and dotted horizontal line denotes 0 mV levels. **(K–M):** A representative still image **(K)** and detected fractional shortening (% FS) along the white line obtained from sites a, b, c, and d in **(L)** are shown in **(M)**. **(M):** The measured % FS was averaged and is shown.

lating blood-derived endothelial progenitor cells [21] or marrow-derived MSCs [2] do not have such high cardiomyogenic differentiation ability. We consequently established a line of EMCs (Fig. 3B, 3D) with a lifespan prolonged by a cell cycle-mediated gene to ensure a supply of cells for analysis. Almost all EMCs beat strongly in a synchronized manner

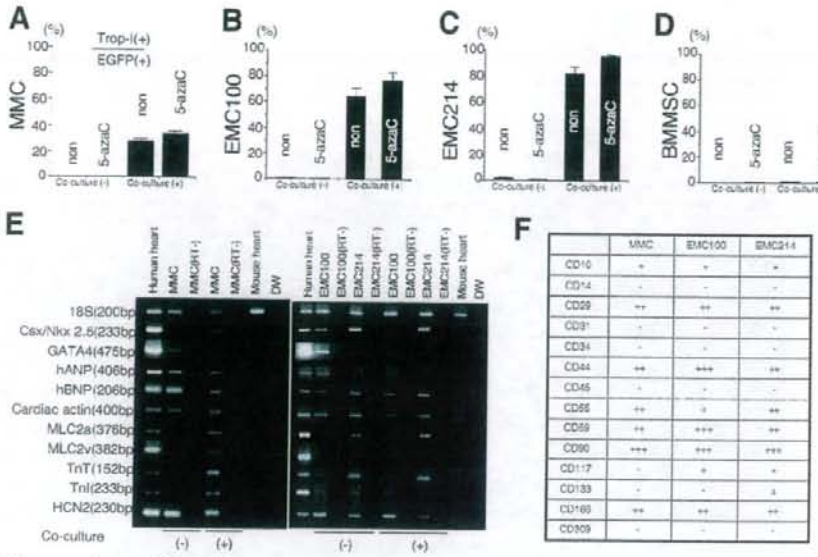

Figure 4. Cardiomyogenic transdifferentiation rates and expression of cardiomyocyte-specific genes and cell surface markers of menstrual blood-derived mesenchymal cells (MMCs) and endometrial gland-derived mesenchymal cells (EMCs). **(A–D):** Cardiomyogenic transdifferentiation rates of MMCs, EMCs, and bone marrow-derived mesenchymal stem cells (BMMSCs). The character in each column denotes pretreatment with 5-azacytidine (5-azaC) or the lack of treatment (non). **(E):** Reverse transcriptase polymerase chain reaction (PCR) was performed with PCR primers with specificity for human genes encoding cardiac proteins but not for the corresponding murine genes (supplemental online Table 1). Human heart and mouse heart cells were used as a positive control and negative control, respectively. Most human cardiac genes were constitutively expressed in the default state of MMCs and EMCs. **(F):** Summary of flow cytometric analysis of MMCs and EMCs with fluorescein isothiocyanate–coupled antibodies against human surface antigens. Abbreviations: DW, distilled water; EGFP, enhanced green fluorescent protein; hANP, human atrial natriuretic peptide; hBNP, human brain natriuretic peptide; HCN2, cyclic nucleotide-gated potassium channel 2; MLC2a, myosin light chain 2a; MLC2V, myosin light chain 2v; TnI, Trop-I, cardiac troponin I; TnT, cardiac troponin T.

(supplemental online Video 1), and 76.4%–96.5% became positive for cardiac troponin-I antibody as a result of cocultivation (Figs. 3A, 3C, 4B, 4C, supplemental online Fig. 2E–2L). EMCs were also positive for sarcomeric α-actinin and connexin 43 (Fig. 2G–2L). APs were recorded from EMCs. The APs obtained from EMCs showed clear cardiomyocyte-specific sustained plateaus and, in some cells, pacemaker potentials (Fig. 3E–3J). The EGFP-positive EMCs contracted simultaneously within the whole visual field (Fig. 3L, 3M). Nuclear fusion between the cocultivated EMC100s or EMC214s and murine cardiomyocytes without separation of the athelocollagen membrane was observed in only 0.57% (6/1058) or 0.28% (5/1758), respectively.

Expression of Cardiomyocyte-Specific Genes and Surface Markers of EMCs and MMCs

The RT-PCR was performed with primers that hybridized with human cardiomyocyte-specific genes but not with the murine orthologs. Differentiated MMCs and EMCs expressed cardiac-specific genes (Fig. 4D). Interestingly, most of the analyzed genes were expressed in the cells before the induction of transdifferentiation by cocultivation.

There is no difference between surface markers of the MMCs and EMCs. Both cells were positive for CD29 (integrin β1), CD59, and negative for CD14, CD34, CD45, CD309 (Flk-1), etc. (Fig. 4E, supplemental online Fig. 3A–3C).

Cardiomyogenic Effects In Vivo

An EGFP-labeled EMC tissue graft made by a novel 3-dimensional cell sheet manipulation [18] was transplanted into male F344 nude rats to ensure in vivo cardiomyogenic transdifferentiation ability. The EGFP-positive cell layer (green) was observed at the epicardial surface of the host heart (Fig. 5B–5D). Whole EMCs throughout the layer expressed a clear striation staining pattern of sarcomeric α-actinin (Fig. 5B–5G), suggesting extremely high cardiomyogenic transdifferentiation ability of EMCs in situ.

MMCs or BMMSCs were transplanted into the nude rats with MI in vivo. Echocardiography showed that the left ventricular fractional shortening (% LVFS) in the MI+MMC group was significantly greater than it in the MI+BMMSC group at 2 weeks after transplantation (Fig. 6A–6I, supplemental online Fig. 4). The MI area was digitized and every 1-mm depth of tissue section stained with Masson's trichrome (Fig. 6J–6O); averaged data are shown in Figure 6P. The MI area was significantly lower in the MI+MMC group than in the MI+BMMSC group. The EGFP-positive mass of MMCs observed in the MI area expressed a clear striation staining pattern of cardiac troponin-I (Fig. 7) and sarcomeric α-actinin (supplemental online Fig. 5), suggesting an extremely high in situ cardiomyogenic transdifferentiation ability of MMCs, which contributed to improvement in cardiac function.

Discussion

Mechanisms of Highly Cardiomyogenic Transdifferentiation Ability of MMCs and EMCs

The gene expression pattern of MMCs and EMCs before cardiomyogenic transdifferentiation is quite different from that of marrow-derived MSCs [2]. GATA-4 expression in the MMCs and EMCs, and Csx/Nkx 2.5 expression in EMCs with the

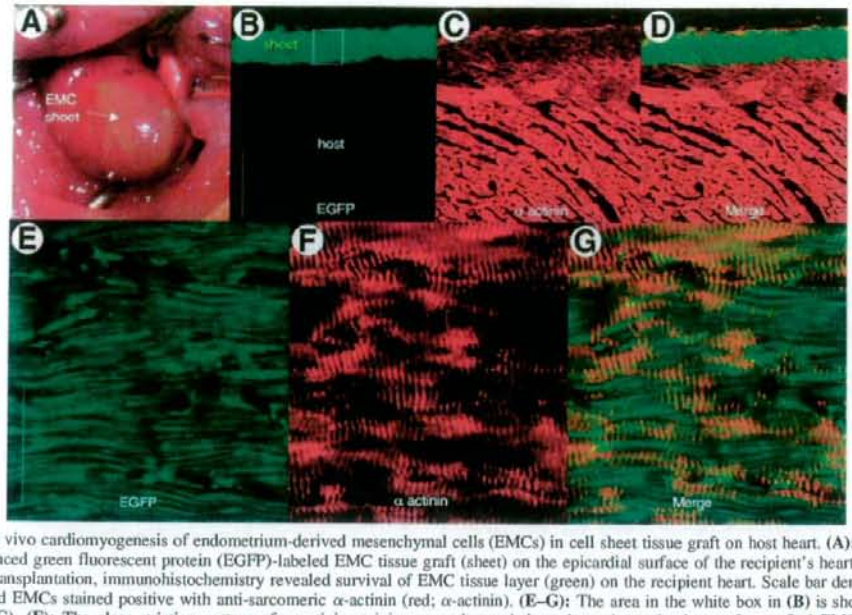

Figure 5. In vivo cardiomyogenesis of endometrium-derived mesenchymal cells (EMCs) in cell sheet tissue graft on host heart. **(A):** Macroscopic view of enhanced green fluorescent protein (EGFP)-labeled EMC tissue graft (sheet) on the epicardial surface of the recipient's heart. **(B–D):** Two weeks after transplantation, immunohistochemistry revealed survival of EMC tissue layer (green) on the recipient heart. Scale bar denotes 100 μm. **(C):** Engrafted EMCs stained positive with anti-sarcomeric α-actinin (red; α-actinin). **(E–G):** The area in the white box in **(B)** is shown in greater detail in **(E–G)**. **(F):** The clear striation pattern of α-actinin staining was observed throughout the entire layer of engrafted EMCs, suggesting extremely high cardiomyogenic potential of EMCs in situ. Scale bar denotes 20 μm.

ability of self-renewal suggest that MMCs and EMCs both have cardiogenic potential and may be termed "cardiac precursor cells" due to their biological features. Cardiac mRNA but not cardiac protein (i.e., troponin-I) was expressed at the default state in the present study, suggesting that both genetic and epigenetic factors may be essential to cause physiologically functioning cardiomyogenic differentiation in MMCs and EMCs. The mechanism of the drastic improvement in the transdifferentiation rate of MMCs and EMCs may be attributable to the default characteristics (expression level of cardiomyocyte-specific mRNA) of MMCs and EMCs in culture compared to marrow-derived MSCs. Highest cardiomyogenic transdifferentiation efficiency was observed in EMC214s (96.5%), EMC100s (76.4%), UCBMSCs (44.9%) [11], MMCs (33.2%), PCPCs (15.1%) [12], and BMMSCs (0.3%, Fig. 4D) [2] in that order. In the practical point of view, EMCs and UCBMSCs are difficult to obtain in enough numbers during the first few passages. MMCs are, therefore, the most suitable cellular source for cardiac stem cell therapy, having a high cardiomyogenic transdifferentiation efficiency. MMCs, EMCs, UCBMSC, and PCPCs are derived from the organ that is related to the pregnancy, therefore the high cardiomyogenic transdifferentiation ability of mesenchymal cells may be caused by a pregnancy-related environmental condition.

Origin of the MMCs and EMCs

Cell surface marker analysis revealed that MMCs are neither encirculating endothelial progenitor cells [22] nor macrophages, but are mesenchymal phenotype cells. We speculated that MMCs may originate in uterine endometrial glands since a lot of detached endometrial glands were observed in menstrual blood and EMCs have the same surface marker as the MMCs, as well as an extremely high cardiomyogenic potential (76.4%–96.5% and 33.2%, respectively). As has been reported, MSCs cannot be detected in circulating blood and all tissues have MSC reservoirs localized in the perivascular niche [23], so EMCs and MMCs do not seem to originate from BMMSCs.

Clinical Contribution

In the present study, MMC transplantation improved impaired cardiac function in vivo. Since MMCs were transplanted at 2 weeks after coronary occlusion, when myocardial necrosis had been completed, the improvement of cardiac function is not due only to transplanted MMC-induced neovascularization [7, 8] or an antiapoptotic [9] effect on infarcted cardiomyocytes. Since they display high cardiomyogenic transdifferentiation ability in vitro and massive cardiomyogenic transdifferentiation in vivo, MMC-derived cardiomyocytes may play a role in the improvement of cardiac function in the present study. Myocardial infarction is known to suppress contraction ability of cardiomyocytes even at normal zone by left ventricular remodeling. Therefore MMC-derived paracrine factors may also play an important role in recovery of % LVFS by prevention of development of LV remodeling.

Neovascularization and the antiapoptotic effect are important for improving cardiac function to some extent. However, the feasible effect is dependent on the number of residual host cardiomyocytes in the infarcted myocardium. To achieve further improvement of cardiac function, a stem cell source that can be expected to exhibit powerful cardiomyogenic transdifferentiation in situ is required. MMCs can be transdifferentiated into cardiomyocytes in situ on the recipient heart, suggesting that they are a promising source for cardiac stem cell-based therapy material, significantly more efficient for cardiomyogenesis than BMMSCs.

MMCs can be readily obtained in a noninvasive manner from young female volunteers, and stored. It should therefore be possible to obtain MMCs of all the HLA types, possibly enabling the establishment of an MMC bank system to facilitate cardiac stem cell-based therapy.

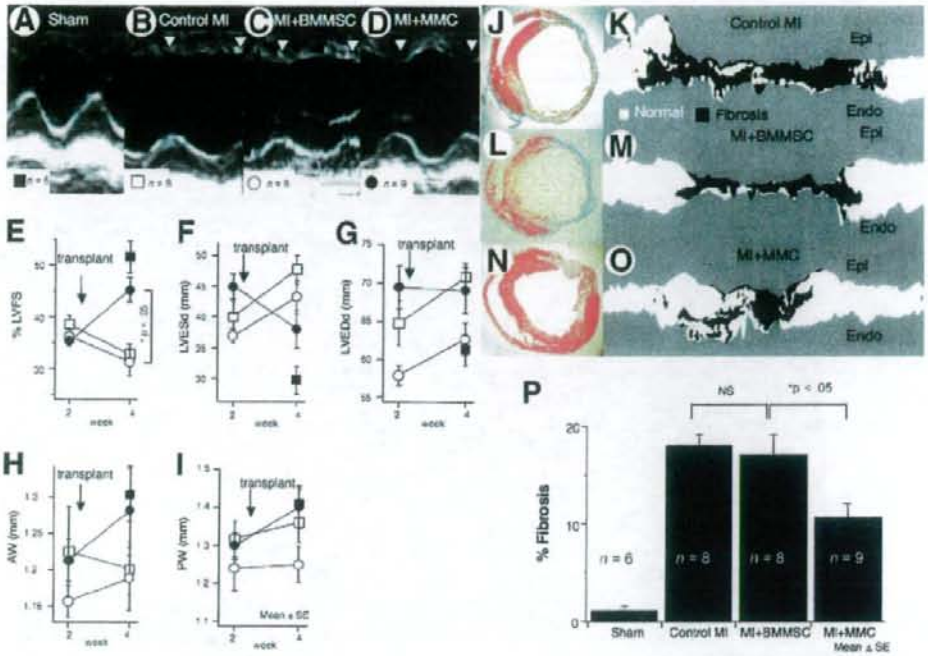

Figure 6. The effect of menstrual blood-derived mesenchymal cell (MMC) transplantation on cardiac function. **(A–D):** Representative M-mode echocardiographic images. The contraction of the left ventricular (LV) anterior wall was improved by transplantation of MMCs (white arrows). The symbol of and number in each group is depicted at the bottom left of each image. **(E–I):** Measured LV parameters are averaged and shown at 2 weeks and 4 weeks after the myocardial infarction (MI). The significant improvement of **(F)** LV end-systolic diameter (LVESd) and **(E)** % fractional shortening (% LVFS) were observed. The diameter of **(H)** anterior left ventricular wall thickness (AW), and **(I)** posterior left ventricular wall thickness (PW). There is no statistical significance. **(J–O):** Representative Masson's trichrome stain images **(J, L, N)** and digitized images **(K, M, O)** of control MI group, MI + bone marrow-derived mesenchymal stem cell (BMMSC), and MI + MMC group are shown. **(P):** The calculated % fibrosis areas are summed and averaged. The MMC transplantation showed significant reduction of % fibrosis area. Abbreviations: Endo, endocardium; Epi, epicardium; NS, not significant.

Role of Established Cardiomyogenic EMC Cell Line for Determining Cardiomyogenic Factors

Several stem cell types are used for clinical patients. Of these, MSCs are reported to show cardiomyogenesis in vitro. Thus, the analysis of key mechanisms for cardiomyogenic differentiation in the human mesenchymal cell is extremely important in order to expand the efficacy of current cardiac stem cell therapy. However, it is very difficult to specify the key factor of cardiomyogenesis by in vivo experiment only. Establishment of EMCs and an in vitro cardiomyogenic differentiation assay system are essential. Stable and high cardiomyogenic transdifferentiation ability in our established system enables us to observe, with wide dynamic range, the effects of treatment for cardiomyogenesis. Moreover, the primary culture condition of murine cardiomyocytes usually fluctuates due to variations in environments, the skill of individual researchers, and institutional differences in isolation protocols. Our established EMCs may provide a good positive control for a cardiomyogenic assay system in vitro to check whether the feeder cell condition is suitable for cardiomyogenic assay. When feeder conditions are suitable, we can survey for possible cardiomyogenic assistant factors or appropriate culture conditions for human BMMSCs by applying various agents or modifying culture conditions systematically. Thus, by using our EMCs and cocultivation system, we may be able to expand the cardiomyogenic differentiation potential of marrow-derived MSCs. Consequently, we may be able to increase the efficacy of cardiac stem cell-based therapy dramatically.

Neither passive stretching of EMCs nor an application of the supernatant of murine cardiomyocyte culture medium to the EMCs alone caused cardiomyocyte differentiation. Taking these findings into account, the multiple environmental factors, including mechanical stretching and/or feeder cardiomyocyte-derived humoral factors, seem to contribute to cardiomyogenic transdifferentiation in human mesenchymal cells. Further experiments should be done.

Study Limitations

Cell fusion between the human cells (MMCs or EMCs) might be a major cause of EGFP-positive cardiomyocytes in the present study. However, EGFP-positive cardiomyocytes could be observed, even when human cells and murine cardiomyocytes were cocultured separately by the athelocollagen membrane that is permeable for only small molecules (less than 5,000 MW)—thus allowing no possible penetration of cells or organelles through the membrane (supplemental online Fig. 6). Furthermore, even if the cells were cocultured without the athelocollagen membrane, nuclear fusion between EMC100s, EMC214s, or MMCs and fetal murine cardiomyocytes was less than 1% in the present study. Moreover, transdifferentiated EMCs at the external layer of the cell sheet graft on the epicardial surface did not directly contact the host cardiomyocytes (Fig. 5). Taking these results

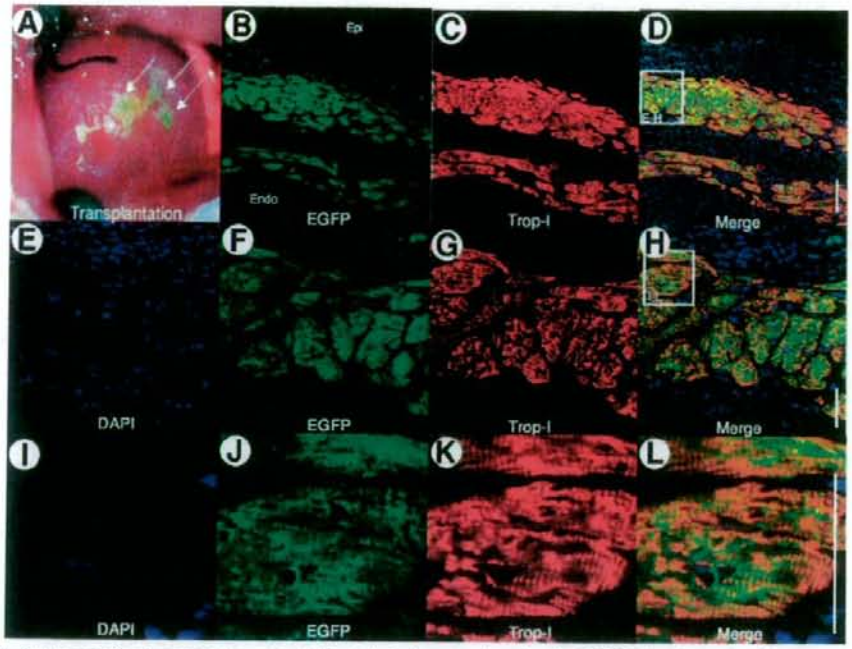

Figure 7. Cardiomyogenesis of engrafted menstrual blood-derived mesenchymal cells (MMCs) in vivo. **(A):** Macroscopic view of the recipient's heart immediately after enhanced green fluorescent protein (EGFP)-labeled MMC transplantation (white arrows) into the myocardial infarction area of the recipient's heart. **(B–L):** Two weeks after transplantation, immunohistochemistry revealed survival of the MMC tissue layer (green) on the treated heart. **(B–D):** Engrafted MMCs stained positive with anti-cardiac troponin-I (red; Trop-1). Scale bar denotes 100 μm. **(E–H, I–L):** The area in the white box in **(D)** was observed in higher resolution **(E–H)** and the white box in **(H)** was also observed in higher resolution **(I–L).** **(K):** The clear striation pattern of Trop-I staining was observed throughout the whole layer of engrafted MMCs, suggesting extremely high cardiomyogenic potential of MMCs in situ. Scale bar denotes 20 μm. Abbreviations: DAPI, 4′-6-diamidino-2-phenylindole; Endo, endocardium; Epi, epicardium.

into account, we concluded that the cell fusion did not play a major role in the observed significant cardiomyogenic potential of MMCs and EMCs in the present study.

Infarcted heart tissue may increase auto-fluorescence in some fixative conditions and such auto-fluorescence of host cardiomyocytes might be confused as EGFP-positive like cells. However, autofluorescence of the host myocardium adjacent to the infarcted area was not significant in our present condition (Figs. 5B, 6B, supplemental online Fig. 5B, 5F). Therefore, EGFP-positive tissue in the present study can be defined as of human cell origin and easily distinguished from the host heart by the EGFP fluorescent intensity.

The transfection of the cell cycle-mediated gene may increase cardiomyogenic differentiation to some extent. However, our previous study in human BMMSCs. [2] with the same combination of cell cycle-mediated gene transfection, did not show any increase in efficiency. Furthermore, non-gene-transfected MMCs have an extremely high cardiomyogenic efficiency compared to gene-transfected BMMSCs. Taking these results into account, we concluded that transfection of those genes does not play an essential role in causing such high cardiomyogenic differentiation efficiency in EMCs.

In comparison to previous papers, there was no observable effect of BMMSC transplantation on cardiac function in the present study. This discrepancy may be caused by different experimental conditions, that is, species difference between BMMSCs and the host animal [24], transplantation at acute myocardial infarction [25–27], and usage of immunosuppressive agents, etc [24–27].

In the present study, we did not use a pressure-tipped catheter, therefore the LV dp/dt value may be underestimated.

Summary

MMC transplantation decreased fibrosis area and restored the LV systolic function in the MI-model in vivo. Engrafted MMC transdifferentiated into cardiomyocyte within MI area. MMC can be a major cell source for stem cell therapy to achieve cardiomyogenesis.

Acknowledgments

The research of N.H. and N.N. was partially supported by a grant from the Ministry of Education, Science and Culture, Japan. A part of this work was undertaken at the Keio Integrated Medical Research Center. We thank M. Uchiyama, A. Furuta, K. Hayakawa, and K. Okamoto for help during the experiments. N.H. and N.N. contributed equally to this work. A part of this work was reported at the annual meeting of the American College of Cardiology 2005, 2006, and 2007.

Disclosure of Potential Conflicts of Interest

The authors indicate no potential conflicts of interest.

REFERENCES

1 Makino S, Fukuda K, Miyoshi S et al. Cardiomyocytes can be generated from marrow stromal cells in vitro. J Clin Invest 1999;103:697–705.
2 Takeda Y, Mori T, Imabayashi H et al. Can the life span of human marrow stromal cells be prolonged by bmi-1, E6, E7, and/or telomerase without affecting cardiomyogenic differentiation? J Gene Med 2004;6: 833–845.
3 Chen SL, Fang WW, Ye F et al. Effect on left ventricular function of intracoronary transplantation of autologous bone marrow mesenchymal stem cell in patients with acute myocardial infarction. Am J Cardiol 2004;94:92–95.
4 Orlic D, Kajstura J, Chimenti S et al. Bone marrow cells regenerate infarcted myocardium. Nature 2001;410:701–705.
5 Wang JS, Shum-Tim D, Galipeau J et al. Marrow stromal cells for cellular cardiomyoplasty: Feasibility and potential clinical advantages. J Thorac Cardiovasc Surg 2000;120:999–1005.
6 Shake JG, Gruber PJ, Baumgartner WA et al. Mesenchymal stem cell implantation in a swine myocardial infarct model: Engraftment and functional effects. Ann Thorac Surg 2002;73:1919–1926.
7 Gojo S, Gojo N, Takeda Y et al. In vivo cardiovasculogenesis by direct injection of isolated adult mesenchymal stem cells. Exp Cell Res 2003; 288:51–59.
8 Tang YL, Zhao Q, Zhang YC et al. Autologous mesenchymal stem cell transplantation induce VEGF and neovascularization in ischemic myocardium. Regul Pept 2004;117:3–10.
9 Gnecchi M, He H, Liang O et al. Paracrine action accounts for marked protection of ischemic heart by Akt-modified mesenchymal stem cells. Nat Med 2005;11:367–368.
10 Kocher AA, Schuster MD, Szabolcs MJ et al. Neovascularization of ischemic myocardium by human bone-marrow-derived angioblasts prevents cardiomyocyte apoptosis, reduces remodeling and improves cardiac function. Nat Med 2001;7:430–436.
11 Nishiyama N, Miyoshi S, Hida N et al. The significant cardiomyogenic potential of human umbilical cord blood-derived mesenchymal stem cells in vitro. STEM CELLS 2007;25:2017–2024.
12 Okamoto K, Miyoshi S, Toyoda M et al. 'Working' cardiomyocytes exhibiting plateau action potentials from human placenta-derived extraembryonic mesodermal cells. Exp Cell Res 2007;313:2550–2562.
13 Terai M, Uyama T, Sugiki T et al. Immortalization of human fetal cells: the life span of umbilical cord blood-derived cells can be prolonged without manipulating p16INK4a/RB braking pathway. Mol Biol Cell 2005;16:1491–1499.
14 Takeuchi M, Takeuchi K, Kohara A et al. Chromosomal instability in human mesenchymal stem cells immortalized with human papilloma virus E6, E7, and Htert genes. In Vitro Cell Dev Biol Anim 2007;43: 129–138.
15 Schwab KE, Gargett CE. Co-expression of two perivascular cell markers isolates mesenchymal stem-like cells from human endometrium. Hum Reprod 2007;22:2903–2911.
16 Meng X, Ichim TE, Zhong J et al. Endometrial regenerative cells: A novel stem cell population. J Transl Med 2007;5:57–66.
17 Kyo S, Nakamura M, Kiyono T et al. Successful immortalization of endometrial glandular cells with normal structural and functional characteristics. Am J Pathol 2003;163:2259–2269.
18 Itabashi Y, Miyoshi S, Kawaguchi H et al. A new method for manufacturing cardiac cell sheets using fibrin-coated dishes and its electrophysiological studies by optical mapping. Artificial Organs 2004;29:95–103.
19 Furuta A, Miyoshi S, Itabashi Y et al. Pulsatile cardiac tissue grafts using a novel three-dimensional cell sheet manipulation technique functionally integrates with the host heart, in vivo. Circ Res 2006;98:705–712.
20 Iijima Y, Nagai T, Mizukami M et al. Beating is necessary for transdifferentiation of skeletal muscle-derived cells into cardiomyocytes. FASEB J 2003;17:1361–1363.
21 Koyanagi M, Urbich C, Chavakis E et al. Differentiation of circulating endothelial progenitor cells to a cardiomyogenic phenotype depends on E-cadherin. FEBS Lett 2005;579:6060–6066.
22 Asahara T, Murohara T, Sullivan A et al. Isolation of putative progenitor endothelial cells for angiogenesis. Science 1997;275:964–967.
23 da Silva Meirelles L, Chagastelles PC, Nardi NB. Mesenchymal stem cells reside in virtually all post-natal organs and tissues. J Cell Sci 2006;119:2204–2213.
24 Wang JA, Fan YQ, Li CL et al. Human bone marrow-derived mesenchymal stem cells transplanted into damaged rabbit heart to improve heart function. J Zhejiang Univ Sci B 2005;6:242–248.
25 Zhang S, Ge J, Sun A et al. Comparison of various kinds of bone marrow stem cells for the repair of infarcted myocardium: Single clonally purified non-hematopoietic mesenchymal stem cells serve as a superior source. J Cell Biochem 2006;99:1132–1147.
26 Grauss RW, Winter EM, van Tuyn J et al. Mesenchymal stem cells from ischemic heart disease patients improve left ventricular function after acute myocardial infarction. Am J Physiol Heart Circ Physiol 2007;293: H2438–H2447.
27 Hou M, Yang KM, Zhang H et al. Transplantation of mesenchymal stem cells from human bone marrow improves damaged heart function in rats. Int J Cardiol 2007;115:220–228.

See www.StemCells.com for supplemental material available online.

Novel Cardiac Precursor-Like Cells from Human Menstrual Blood-Derived Mesenchymal Cells

Naoko Hida, Nobuhiro Nishiyama, Shunichiro Miyoshi, Shinichiro Kira, Kaoru Segawa, Taro Uyama, Taisuke Mori, Kenji Miyado, Yukinori Ikegami, ChangHao Cui, Tohru Kiyono, Satoru Kyo, Tatsuya Shimizu, Teruo Okano, Michiie Sakamoto, Satoshi Ogawa and Akihiro Umezawa

Stem Cells 2008;26;1695-1704; originally published online Apr 17, 2008;
DOI: 10.1634/stemcells.2007-0826

OPEN ACCESS Freely available online

PLoS one

Gremlin Enhances the Determined Path to Cardiomyogenesis

Daisuke Kami[1,3], Ichiro Shiojima[4], Hatsune Makino[1], Kenji Matsumoto[2], Yoriko Takahashi[1], Ryuga Ishii[1], Atsuhiko T. Naito[4], Masashi Toyoda[1], Hirohisa Saito[2], Masatoshi Watanabe[3], Issei Komuro[4], Akihiro Umezawa[1]*

1 Department of Reproductive Biology, National Institute for Child Health and Development, Tokyo, Japan, 2 Department of Allergy and Immunology, National Institute for Child Health and Development, Tokyo, Japan, 3 Laboratory for Medical Engineering, Division of Materials Science and Chemical Engineering, Graduate School of Engineering, Yokohama National University, Yokohama, Japan, 4 Department of Cardiovascular Science and Medicine, Chiba University Graduate School of Medicine, Chiba, Japan

Abstract

Background: The critical event in heart formation is commitment of mesodermal cells to a cardiomyogenic fate, and cardiac fate determination is regulated by a series of cytokines. Bone morphogenetic proteins (BMPs) and fibroblast growth factors have been shown to be involved in this process, however additional factors needs to be identified for the fate determination, especially at the early stage of cardiomyogenic development.

Methodology/Principal Findings: Global gene expression analysis using a series of human cells with a cardiomyogenic potential suggested *Gremlin* (*Grem1*) is a candidate gene responsible for *in vitro* cardiomyogenic differentiation. Grem1, a known BMP antagonist, enhanced DMSO-induced cardiomyogenesis of P19CL6 embryonal carcinoma cells (CL6 cells) 10–35 fold in an area of beating differentiated cardiomyocytes. The Grem1 action was most effective at the early differentiation stage when CL6 cells were destined to cardiomyogenesis, and was mediated through inhibition of BMP2. Furthermore, BMP2 inhibited Wnt/β-catenin signaling that promoted CL6 cardiomyogenesis.

Conclusions/Significance: Grem1 enhances the determined path to cardiomyogenesis in a stage-specific manner, and inhibition of the BMP signaling pathway is involved in initial determination of Grem1-promoted cardiomyogenesis. Our results shed new light on renewal of the cardiovascular system using Grem1 in human.

Citation: Kami D, Shiojima I, Makino H, Matsumoto K, Takahashi Y, et al. (2008) Gremlin Enhances the Determined Path to Cardiomyogenesis. PLoS ONE 3(6): e2407. doi:10.1371/journal.pone.0002407

Editor: Hernan Lopez-Schier, Centre de Regulacio Genomica, Spain

Received January 15, 2008; **Accepted** May 5, 2008; **Published** June 11, 2008

Funding: This study was supported by a grant from the Ministry of Education, Culture, Sports, Science and Technology (MEXT) of Japan and Health and Labor Sciences Research Grants; by a Research grant on Health Science Focusing on Drug Innovation from the Japan Health Science Foundation; by the Program for Promotion of Fundamental Studies in Health Science of the Pharmaceuticals and Medical Devices Agency; by a grant from the Terumo Life Science Foundation; by a Research Grant for Cardiovascular Disease from the Ministry of Health, Labor and Welfare (MHLW); and by a Grant for Child Health and Development from the MHLW.

Competing Interests: The authors have declared that no competing interests exist.

* E-mail: umezawa@1985.jukuin.keio.ac.jp

Introduction

The critical event in heart formation is commitment of mesodermal cells to a cardiomyogenic fate and their migration into anterolateral regions of the embryo during late gastrulation. In this process, morphogenic movements and cardiac fate determination are regulated by cytokines such as bone morphogenetic proteins (BMPs) [1–3], and fibroblast growth factors (FGFs) [4–7]. These secreted proteins from neighboring endoderm, ectoderm, and the mesoderm itself, play important roles in induction of cardiac transcription factors [8] and differentiation of cardiomyocytes in amphibians [9] and avians [4]. Cardiomyogenic signals, such as BMPs and FGFs, indeed activate expression of cardiac specific transcriptional factors (Csx/Nkx2.5, Gata4, Mef2c), and these transcriptional factors activate expression of circulating hormones (atrial natriuretic peptide (ANP), brain natriuretic peptide (BNP)), and cardiac specific proteins (myosin heavy chain (MyHC), myosin light chain (MyLC)). Wnt family proteins, cysteine-rich, and secreted glycoproteins, have also been implicated in embryonic development [10,11], and cardiomyogenesis [12,13]. In *Drosophila*, '*wingless*', a homologue of vertebrate Wnt is involved in expression of '*tinman*', a *Drosophila* homologue of Csx/Nkx2.5, through '*armadillo*', a *Drosophila* ortholog of β-catenin, and drives heart development [14]. In vertebrates, however, Wnt1/3a, which activates the canonical Wnt/β-catenin signaling pathway leading to stabilization of β-catenin as a downstream molecule through inactivation of glycogen synthase kinase-3β, inhibits cardiomyocytic differentiation from cardiac mesoderm [15–18]. Wnt11 promotes cardiac differentiation via the non-canonical pathway in *Xenopus* [12] and murine embryonic cell lines [19]. The secretion of Wnt inhibitors such as 'Cerberus', 'Dickkopf' and 'Crescent' by the anterior endoderm prevents Wnt3a secreted by the neural tube from inhibiting heart formation [15–17].

In this study, we performed GeneChip analysis to identify multiple extracellular determinants, such as cytokines, cell

membrane-bound molecules and matrix responsible for cardiomyogenic differentiation, and evaluated the statistical significance of differential gene expression by NIA array analysis (http://lgsun.grc.nia.nih.gov/ANOVA/) [20], a web-based tool for microarray data analysis. We found that Grem1 enhances the determined path to cardiomyogenesis in a stage-specific manner, and that inhibition of the BMP signaling pathway is, at least in part, involved in initial determination of Grem1-promoted cardiomyogenesis.

Results

GeneChip and statistical analysis

To identify cytokines and transcription factors responsible for cardiomyogenic differentiation, 69 human cells were analyzed, depending on gene expression levels, by GeneSpringGX software, and clustered into 30 groups (Fig. 1A, Table 1). Among the 30 groups, 21 groups included cells with a cardiomyogenic potential (Fig. 1B: red numbers). To identify genes specific for these groups, hierarchical clustering was employed, using the average distance method. Genes with the lowest average expression E(G1) within the cluster that can differentiate into cardiomyocytes and genes with the highest average expression E(G2) outside the cluster were identified, as previously described [20–22]. Genes which have E(G1)>E(G2) were estimated, using the False Discovery Rate (FDR<0.05). Grem1 was nominated as a cluster-specific cardiomyocyte-promoting gene in cells that could differentiate into cardiomyocytes following NIA array analysis (Fig. 1B). The gene expression profile reported in this paper has been deposited in the Gene Expression Omnibus (GEO) database (http://www.ncbi.nlm.nih.gov/geo: accession no. GSE8481, GSM41342-GSM41344, and GSM201137- GSM201145).

Cardiomyogenic differentiation of CL6 cells with Grem1 and DMSO

To investigate cardiomyogenic activity of Grem1, P19CL6 embryonal carcinoma cells (CL6 cells) were used for assessment of *in vitro* cardiomyogenic differentiation, since CL6 cells are reproducibly and stably induced into beating cardiomyocytes by DMSO (Fig. 2Aa) [23]. CL6 cells did not differentiate following exposure to Grem1 alone at concentrations of 63 or 125 ng/ml for 14 days (Fig. 2B). However, Grem1 dramatically promotes DMSO-induced cardiomyogenic differentiation at a concentration of 63 and 125 ng/ml; Grem1 (125 ng/ml) especially increased DMSO-induced cardiomyogenic differentiation of CL6 cells as assessed by beating area (Fig. 2Ab and B) (Movie S1 and S2, http://1954.jukuin.keio.ac.jp/umezawa/kami/index.html).

RT-PCR of differentiated or undifferentiated CL6 cells

To investigate gene expression as well as morphological analysis, i.e. beating, during cardiomyogenic differentiation, RT-PCR analysis was performed to detect expression of cardiomyocyte-specific/associate transcription factors, and structural genes (Fig. 2C). Genes encoding *Csx/Nkx2.5*, *Gata4*, *Hand2*, *Mef2c*, *ANP*, *BNP*, *MyLC-2a*, *MyLC-2v*, and *β-MyHC* were up-regulated during cardiomyogenic differentiation of CL6 cells treated with Grem1 and DMSO (Fig. 2C: lanes 6, 7 versus lane 3). Triplicate independent experiments confirmed the concentration-dependent Grem1 action on cardiomyogenic differentiation. The cardiomyocyte-specific genes (*Csx/Nkx2.5*, *Gata4*, *MyLC-2a*, *MyLC-2v*) expression level of CL6 cells treated with DMSO and Grem1 (63 and 125 ng/ml) were also the same as or higher than that of DMSO-induced CL6 cells by semi-quantitative RT-PCR (Figure S1).

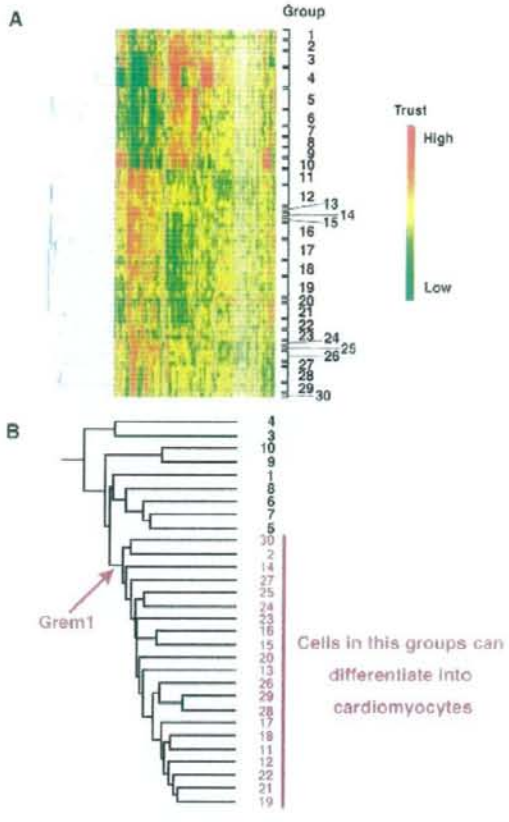

Figure 1. Hierarchical clustering analysis on cultured human cells. (A) Hierarchical clustering analyzed by GeneSpring. Based on gene expression pattern, 69 human cells were clustered into 30 subgroups. The raw data from the GeneChip analysis are available at the GEO database with accession number GSE8481, GSM41342- GSM41344, and GSM201137- GSM201145. **(B)** Hierarchical clustering analysis was performed by NIA array (http://lgsun.grc.nia.nih.gov/ANOVA/), using averaged values of 30 sub-groups. Among the 30 groups, 21 groups included cells with a cardiomyogenic potential. To identify genes specific for these groups, hierarchical clustering was employed. *Grem1* was nominated as a cluster-specific cardiomyocyte-promoting gene in cells that could differentiate into cardiomyocytes.
doi:10.1371/journal.pone.0002407.g001

Immunocytochemistry of differentiated or undifferentiated CL6 cells

To examine CL6 cells for expression of cardiomyocytic protein, immunocytochemical analysis was performed. CL6 treated with Grem1 (125 ng/ml) and DMSO exhibited clear striation with immunostain using anti-cTnT or anti-α-actinin (Fig. 2Da and b). The MF20- and cTnT-positive cells after exposure to Grem1 and DMSO formed clusters (Fig. 2Ea), compared with the cells after exposure to DMSO alone (Fig. 2Eb). CL6 cells treated with Grem1 alone were negative for MF20 and cTnT, but became positive for both markers following exposure to Grem1 (63 and 125 ng/ml) and DMSO (Fig. 2F). The beating area (Fig. 2B) showed a tendency similar to the MF20- and cTnT-positive area (Fig. 2F), thus there were positive correlations between them.